THESIS FOR THE DEGREE OF DOCTOR OF PHILOSOPHY (PH.D)

EXPERIMENTAL OPHTHALMOLOGY – *EX VIVO* MODELLING OF NEOVASCULAR DISEASES IN OPHTHALMOLOGY

by
Lyubomyr Lytvynchuk, MD

Supervisor:

Prof. Goran Petrovski, MD, PhD, Dr habil

UNIVERSITY OF SZEGED
DOCTORAL SCHOOL OF
CLINICAL MEDICINE
DEPARTMENT OF OPHTHALMOLOGY

SZEGED, 2020

to my parents, Marta and Mychailo

CONTENTS

ABBREVIATIONS:

AMD	Age-related macular degeneration
anti-VEGF	Vascular endothelial growth factor antagonists
BRB	Blood-retinal barrier
BSS	Balanced salt solution
CNV	Choroidal neovascularization
DNA	Deoxyribonucleic acid
FA	Fluorescein angiography
FAZ	Fovea avascular zone
FVP	Fibrovascular proliferation
G	Gauge
HN	Hypodermic needle
hrs	Hours
iSD-OCT	Intraoperative spectral domain optical coherence tomography
NV	Neovascularization
OCT	Optical coherence tomography
PDR	Proliferative diabetic retinopathy
PEDF	Pigment epithelium-derived factor
PKI	Polykaryocytic indices
PM	Pathologic myopia
VEGF	Vascular endothelial growth factor
VEGFA	Vascular endothelial growth factor A
VEGFR2	Vascular endothelial growth factor receptor 2

MAGYAR NYELVŰ ÖSSZEFOGLALÓ

Az IVI technika szubkután vagy spinális érzéstelenítő tűk használata miatt a szemrétegek (kötőhártya, sclera, ciliáris test) károsodásához vezet. Emellett, a tűnyíláson megragadó sejtes és egyéb fertőzéshez vezető anyagok is az üvegtesti térbe kerülhetnek. Adataink alátámasztják azt a hipotézist, mely szerint az IVI-hez rutinszerűen használt szubkután tűk belső éle sejteket vághat ki útja mentén, patkányból- és kadaverekből származó szemekbe történő injektáláskor. A tű átmérője befolyásolja a szövetkárosodás mértékét, valamint az injektált anyag megfelelő eloszlását. A tű hegyének kialakítása pedig meghatározza az injekció beadási helyének formáját és az esetleges üvegtesti refluxot. Tanulmányunk azt támasztja alá, hogy a 30G hipodermikus tűk kisebb szövetkárosodást okoznak, mint a hipodermikus 27G, valamint a Pencan 27G tűk.

A kiváltott immunreakció vizsgálatakor figyelembe kell venni az injekció során az üvegtesti térbe kerülő sejtes/ szöveti anyag, valamint az IVI-val beadott hatóanyag szerepét is. Szem előtt kell tartani azt is, hogy a betegek kezelésekor, a ranibizumab, bevacizumab, pegaptanib és aflibercept különböző koncentrációban a sejtek túlélését és mitózisát is gátolja. A vizsgált anti-VEGF készítmények közül a ranibizumab gátolta legkevésbé a proliferációt, ezzel ellensúlyozva az apoptózist.

Többmagvú óriássejtek teljesen eltűntek 10 és 100 µg/ ml koncentrációjú aflibercept jelenlétében tenyésztett L_{929} sejtkultúrákból, mely a készítmény sejtmembrán és sejtmag közötti jelátvitelre kifejtett hatását jelezheti. A gyógykészítményekkel feltárt eredmények, valamint egyéb szerepük további vizsgálatot igényel *in vitro* és *in vivo*.

Emellett, az anti-VEGF készítmények hormetikus hatásának vizsgálatához, a retinára kifejtett egyéb kedvezőtlen hatások felderítéséhez, kiküszöböléséhez, több tanulmányra van szükség.

1. Introduction

The visual system plays one of the most important roles in mammals for orientation in the environment and therefore survival. In humans, the visual system is even more important, as almost every type of activity necessitates visual input. With its anterior and posterior segments, the eyes serve as the organs for receiving, conducting and processing of visual information. The eyes are responsible for the perception and transmission of visual information to the visual cortex through nerve impulses. The visual cortex finally interprets such information and transforms it into images of the surrounding environment (Levin 2011).

Among other sensory organs of the human body, the eyes are clearly the most complex and delicate in their structure and function, which is enabled by a process of highly complex embryological development (**Figure 1**). In order to perceive and transmit a sharp image to the visual cortex, the optic media should be perfectly clear, while the multifunctional posterior layers should be unimpaired on both eyes simultaneously. The structure of the human eye is divided into anterior and posterior segments accordingly (**Figure 1**).

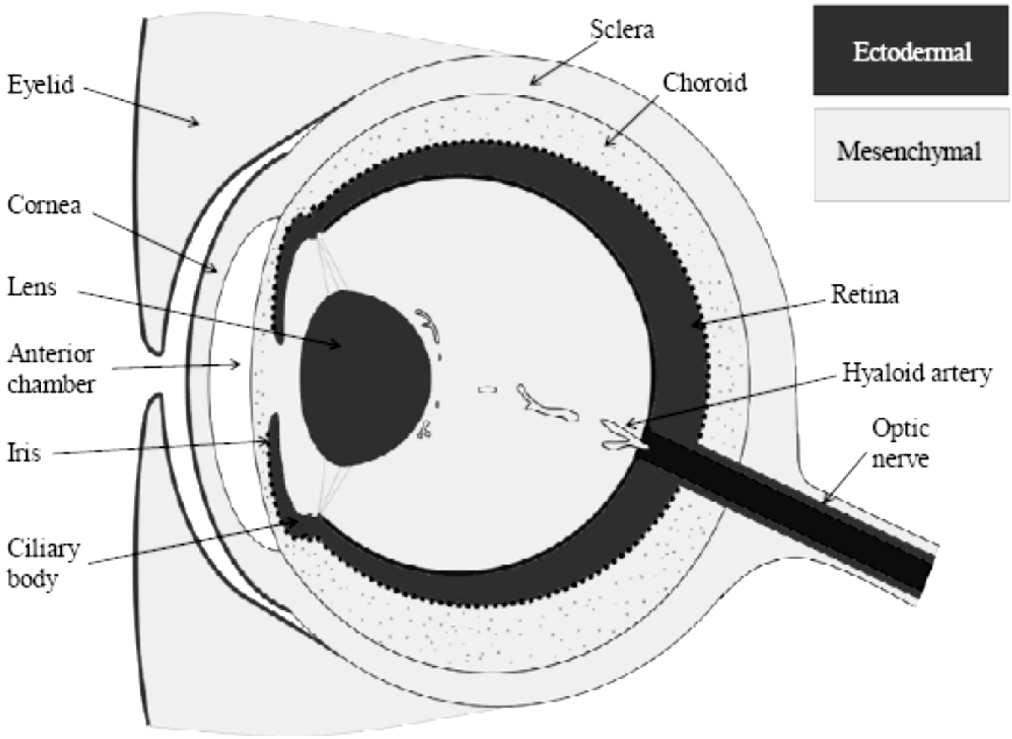

Figure 1. Development of the eye and its segments (Petrovski et al., book chapter in Autophagy: Principles, Regulation and Roles in Disease, 2012, Nova Publishers).

The anterior segment of the eye consists of the cornea, iris, ciliary body and the crystalline lens. The posterior segment is covered from the outside by the sclera, and includes the choroid, retina and vitreous body. The retina itself can be divided into its central part - macula, and peripheral retina. The macula and its central portion – the *fovea centralis*, are responsible for the central, color, and sharp vision, while the peripheral retina is responsible more for visual field and orientation (**Figure 2**).

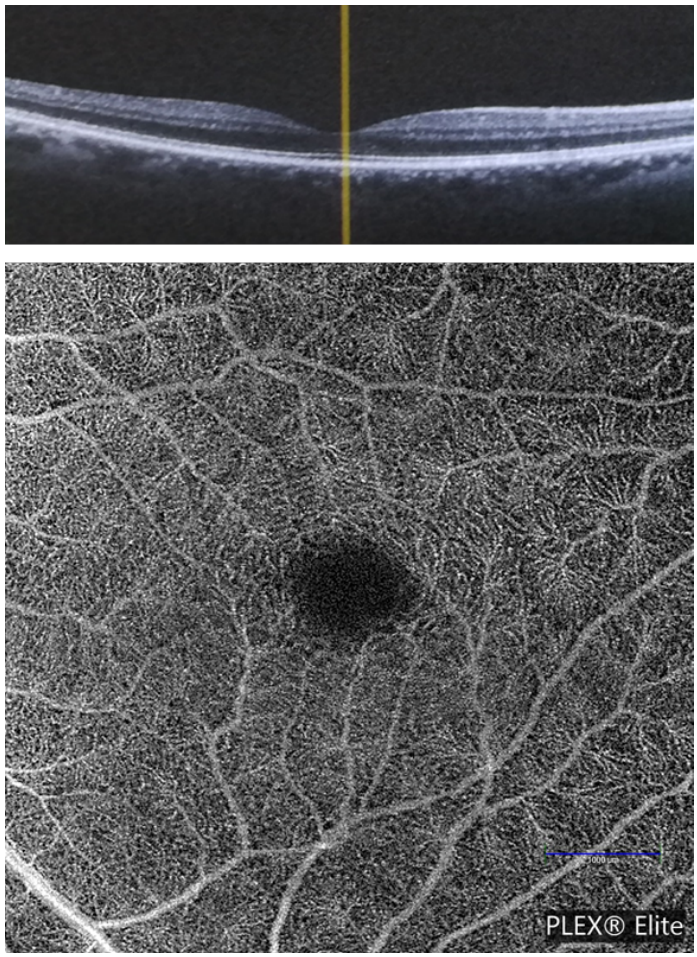

Figure 2. Optical coherence images (OCT) images of the macular region of the normal human retina (upper panel: vertical line marks the central retina – the fovea) with OCT angiography of the deep vascular layer of the retina (lower panel: the avascular central part represents the fovea avascular zone (FAZ)).

The retina with its highly differentiated ten layers fulfills probably the most important function in the eye and is therefore, very sensible to any structural changes. The development of pathological processes typically spread within the planes of anatomical barriers. The extension and shape of intraretinal hemorrhages, infarcts and exudates can be explained by the presence of different horizontal and vertical

structural planes in the retina. Foremost, the ischemic changes caused by the insufficient blood flow and/or atrophic, degenerative or inflammatory changes have been shown to lead to a break in one of the anatomical barriers and development of different complications, including fibrovascular proliferations (Naumann 2007).

The macula and its very central portion – the *fovea centralis* (including the foveola) provide the most significant function of the visual perception. That is why the development of pathological lesions within this area makes a crucial impact on the central visual function. In healthy or physiological conditions, the retinal vascular system remains unimpaired due to an existing balance between angiostatic and angiogenic factors that have been produced by the intraocular tissues. The ischemic and inflammatory processes within the ocular tissues can increase the need of oxygen and lead to a balanced change with the prevalence of angiogenic factors that are produced by the compromised and damaged cells. However, not only increase of the concentration of angiogenic factors can predispose to neovascularizations (NVs), but decrease in the concentration of angiostatic factors as well. To prevent the development of NVs, beside the active components (angiostatic proteins), there are also passive stabilizing components that belong to the extracellular matrix (collagens, elastins, fibrin constitute and the like). The insufficient protective abilities of both active and passive components result in the fundamental pathophysiologic condition known as breakage of the inner- or outer- blood-retinal barrier (BRB), which is common for almost every NV-eye disease. The integrity of BRB is provided by the presence of adhesion proteins called cadherins that build up the vascular endothelial boundaries. The growth of the new vessels can arise only when the tight junctions – the cadherins are degraded. Vascular endothelial growth factor (VEGF) was identified as one of the most important angiogenic factors, because the binding of this factor to the VEGFR-2 receptor on the cell surface actually leads to degradation of the tight junctions and opening of the BRB. There are a number of other important factors and components that are involved in the breakdown of BRB, including angiopoietin-1, angiopoietin-2, transforming growth factor β and the like. These factors were not in the focus of the current study and were not the subject of discussion here.

One of the most sight threatening complications that can exacerbate the progression of widespread proliferative retinal diseases is the development of sub-, intra- and/or epi- retinal fibrovascular proliferations (FVPs). The dramatic consequences of the eye diseases that are linked to the retinal or choroidal

angiogenesis are responsible for the development of the majority of complications which end up with blindness and handicap. Among these eye diseases that are associated with disruption of the stable state of the vascular system are age-related macular degeneration (AMD), pathologic myopia (PM), angioid streaks, choroidal rupture, chorioretinitis, proliferative diabetic retinopathy and many other diseases of the posterior pole. Ischemia plays a major role in the course of these diseases and serves as an activating mechanism to provoke the splash of NVs. Primary hypoxia, alterations of the vascular perfusions and different compensatory reactions of the vascular bed belong to the other important co-factors of NV-development. Ischemic NV of the retina can originate either from the retinal arteries or the choriocapillary layer. Choroidal neovascularization (CNV) is a common complication caused by the breakdown of the outer BRB, and is one of the most sight threatening complications among the devastating retinal diseases (**Figure 3**).

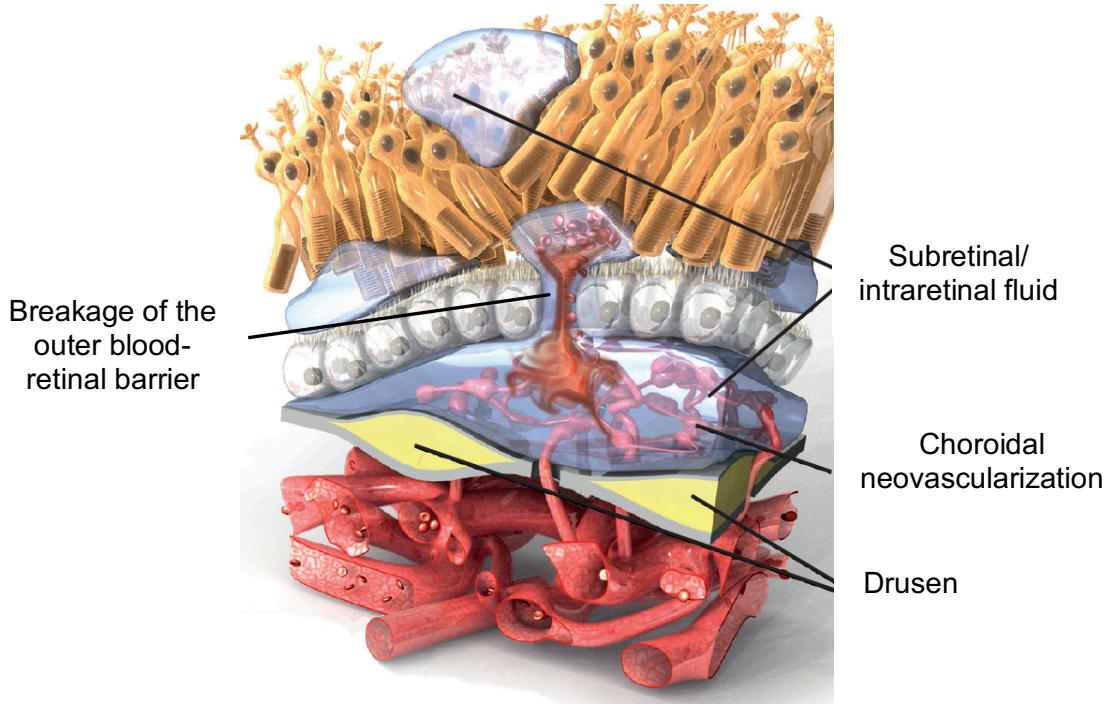

Figure 3. Development of choroidal neovascularization (CNV) as a result of chronic retinal ischemia and breakage of the outer blood-retinal barrier. (Modified from The Angiogenesis Foundation (http://www.scienceofamd.org/wpcontent/uploads/2012/04/Science_of_AMD%20Patient_Brochure.pdf)).

There are a number of treatment modalities to approach the CNV, including the use of laser energy and pharmacotherapy. However, due to the very central location of the CNV (foveal or extrafoveal), the use of laser is sometimes contraindicated, as it

can damage the residual surrounding healthy retina. In the past two decades, the use of pharmacotherapy has radically changed the philosophy of CNV treatment allowing for control and, in some cases, eradication of NV growth.

New drugs that block the VEGF and its receptors (anti-VEGFs) are under constant development and modification, and are widely used to treat CNVs and FVPs. The drug delivery routes are also under rapid development, aiming to transport the drugs or the target molecules exactly where needed. Many preclinical studies and clinical trials have been conducted with the aim to find the most efficient and safe dose-regimens as well as administration techniques.

Since decades, the intravitreal injections (IVI) have become the most common drug delivery method for targeting intraocular diseases associated with increased concentration of VEGF inside the eye (**Figure 4**). The numbers of IVIs performed worldwide are increasing every year, with a great diversity of approaches of giving IVIs being practiced worldwide (Jeganathan and Verma 2009, Scott and Bressler 2013, Avery, Bakri et al. 2014, Ruiz-Moreno, Montero et al. 2015). IVIs facilitate the achievement of immediate therapeutic concentrations of the drug in the eye with decreased or minimal systemic exposure

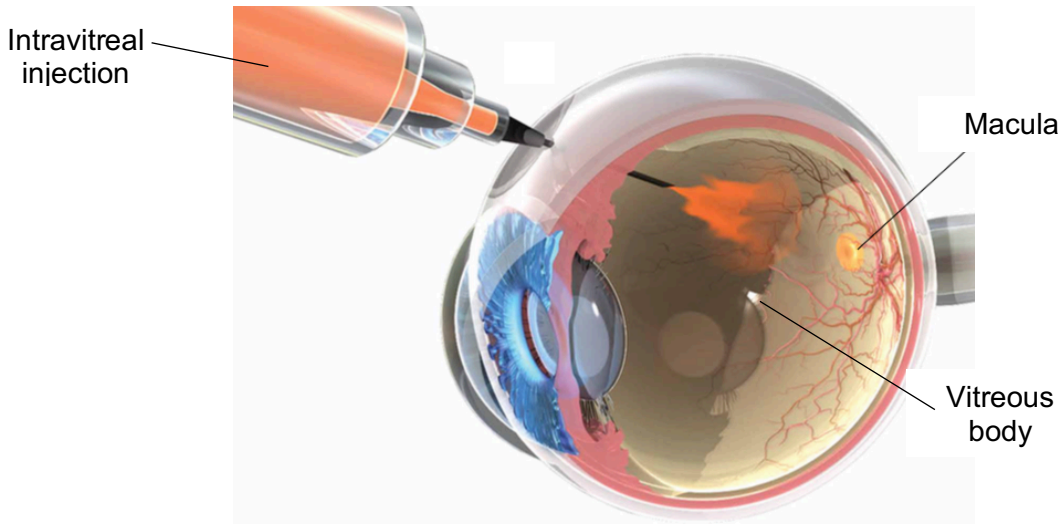

Figure 4. Intravitreal injection (IVI) of drugs into the vitreous body. (Modified from The Angiogenesis Foundation (http://www.scienceofamd.org/wp-content/uploads/2012/05/Science_of_AMD-Wet_AMD_Progression_and_Treatment_Poster.pdf).

A relatively rapid elimination of the injected drug from the vitreous body usually limits the therapeutic efficacy. Repeated injections are able to maintain therapeutic

concentrations in the eye. Numerous studies that analyze the IVI efficacy demonstrate both therapeutic success and risks of complications (van der Reis, La Heij et al. 2011, Avery, Bakri et al. 2014). Every IVI is associated with risk of intraocular inflammation, cataract formation, retinal detachment, intraocular bleeding and other less studied side effects of the anti-VEGF drugs. Intraocular inflammation can be presented with an aseptic or septic inflammation with a rapid or gradual progression. Septic intraocular inflammation – endophthalmitis, remains the most severe post-IVI complication (ranging from 0.018% to 1.4% of the cases), that can lead to a dramatic vision loss and even loss of the eye (Fintak, Shah et al. 2008, Diago, McCannel et al. 2009, Klein, Walsh et al. 2009, Sigford, Reddy et al. 2015). Non-infectious intraocular inflammation or endophthalmitis has been described as well (Jonas, Spandau et al. 2007, Goldberg, Shah et al. 2014). Nevertheless, the true causes or the origin of endophthalmitis have not been studied well. According to some studies, the use of antibiotic eye drops before and after IVIs does not prevent, but can increase the risk of endophthalmitis, while repeated administration of antibiotics can initiate the mutation of the microorganisms to antibiotic-resistant strains (Bhatt, Stepien et al. 2011, Cheung, Wong et al. 2012, Goldberg, Shah et al. 2014). From one aspect, the rate of endophthalmitis is relatively low, but from another, this very complication can cause irreversible sight-threatening condition in the eye. The impact of the different IVI techniques and approaches on the complications' rate is not well studied either (de Caro, Ta et al. 2008, De Stefano, Abechain et al. 2011, Friedman, Lindquist et al. 2014). The role of the needle types used for IVIs is not clear, and for that matter, has not been discussed enough.

It was demonstrated that the thinner needles cause less sclera damage and consequently less vitreous prolapse. The hypodermic (subcutaneous) needles (HN) have been used for IVI, which independent from the diameter of the needle have a trephine-like configuration of the needle tip. During manufacturing, needle tips are polished with a polishing wheel under a certain angle, which makes the outer- and inner- edges of the tip very sharp (Kucklick 2006). This design is widely used for the fine needle aspiration technique, as it facilitates the cut and aspiration of a cellular column of penetrated tissues. That is why the risk of unintended injection of needle cellular content into the vitreous during IVI is high, and the intraocular reaction caused by these cells can be potentially harmful and unpredictable. Foremost, the vitreous body can react to such cells by an autoimmune inflammatory reaction. Additionally,

and probably more dangerous is the presence of persisting superficial or intracellular infections that can contaminate the vitreous body and cause a severe endophthalmitis with unusual clinical presentation. It has been shown that *Chlamydia species* can inhabitate the intracellular space of the conjunctival epithelial cells and remain intact during routine disinfection of the conjunctival sac (Ojcius, Souque et al. 1998, Natividad, Freeman et al. 2010). The autologous cells or microorganisms injected into the vitreous body thus may be a predisposing condition for growth, as the vitreous is a rich natural cultivation medium for such cells (Forrester, Docherty et al. 1986). The presence of multiple regulating factors can either stimulate proliferation of the cells or inhibit it. Hence a potential risk associated with proliferation, and septic or aseptic (autoimmune or of unknown etiology, respectively) inflammation exists.

During IVI, the intraocular pressure is transiently increased. In spite the fact that the IVI site is very tiny and sometimes barely visible, the subconjunctival reflux of the injected drug or the vitreous takes place due to incomplete self-sealing and transient intraocular hypertension. Moreover, the IVI can be associated with pain and bleeding, which can serve as supportive factors of inflammation (Rodrigues, Grumann et al. 2011, Brodie, Ruggiero et al. 2014). The site of IVI, namely the insertion point, as well as the extent of the subconjunctival reflux, usually dependent upon the amount of injected drug, the IVI technique, type of the needle and the vitreous state (Brodie, Ruggiero et al. 2014). The techniques used for delivering IVIs and the needle size can be responsible for the increased risk of contamination. The size and the shape of the entry site after IVI play an important role in the self-sealing and making the eye a closed system again.

For these reasons, the study of conventional technique IVI technique remains in the focus in order to reveal potentially dangerous aspects of this method and ways to improve it.

The efficacy of the IVI of different antivascular drugs (anti-VEGFs) in the treatment of CNVs is well studied and documented in many experimental and clinical studies (Grisanti and Ziemssen 2007, Kumaran, Sim et al. 2009, Biswas, Sengupta et al. 2011, Browning, Kaiser et al. 2012). The data of these studies almost fully explain the complex and multileveled mechanism of anti-VEGF drugs. To the main therapeutic routes of anti-VEGF action belong the following mechanisms: binding of various types of VEGF molecules, downregulation of permeability of NV capillary network and reduction of the persistent edema. Interestingly, data obtained from OCT and

fluorescein angiography (FA) in patients with CNV treated with IVI of anti-VEGF drugs demonstrated a decrease of CNV size and, in certain cases, complete involution (**Figure 5**).

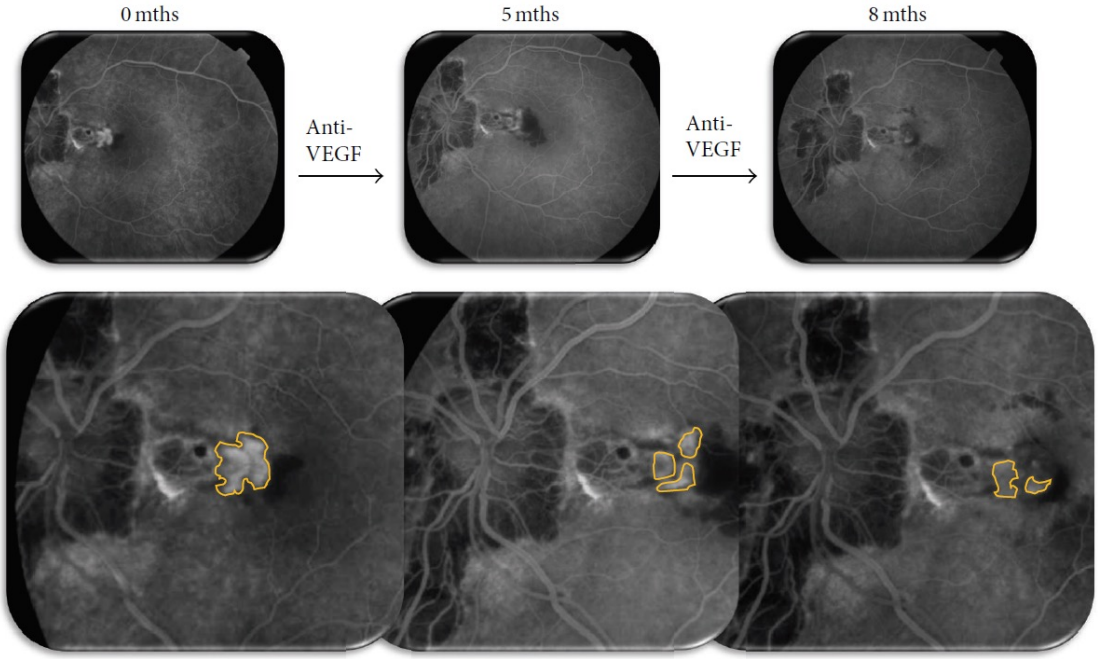

Figure 5. Choroidal neovascularization (CNV) dynamics after repeated anti-VEGF therapy (CNV size is circumscribed with yellow color; images shown are at the 40th second of fluorescein angiography).

It is not completely clear, however, which mechanism of the anti-VEGF pharmacoactivity leads to the regression of CNV dimensions. The cellular matrix of CNVs consists primarily of fibroblasts, myofibroblasts and in general fibroblast-like cells. These types of cells possess a highly active proliferative and mitotic activity (Schnichels, Hagemann et al. 2013). Recent reports have demonstrated data about different mechanisms of influence of anti-VEGF drugs upon different cellular cultures *in vitro*, as well as the duration of drug action and elimination (Wang, Fei et al. 2004, Spitzer, Wallenfels-Thilo et al. 2006, Martin S. Spitzer 2007, Kaempf, Johnen et al. 2008, Carneiro, Falcao et al. 2009, Schnichels, Hagemann et al. 2013). There is a lack of evidence, however, regarding the antiproliferative properties of anti-VEGF drugs, while the significance of the topic is gaining importance with the increase of the number of IVIs instilled worldwide.

2. Aims of the study

1. To examine the amount and content of cellular material being cut during IVI by the needle tip using three different needle types, and accordingly, examine the material that potentially is injected into the vitreous body after transconjunctival penetration in rats and human cadaver eye.

2. To identify the cells and cellular complexes within the cellular content using cyto-histological analysis.

3. To compare the structure of the entry sites (wound structure) of the conjunctiva-sclera-ciliary body tissue complex after different needle types are used.

4. To cultivate *ex vivo* the cell extracts from the needle tips aspirates and to evaluate the proliferative potential of these cells.

5. To investigate the possible side effects of four available anti-VEGF drugs regarding their antiproliferative and apoptotic effects on fibroblast-like cell strain in an *in vitro* model for CNV cellular matrix formation.

6. To analyze the activity of different anti-VEGF drugs upon the antiproliferative and apoptotic activity in regards to dose-dependence.

7. To determine alternative cell survival or death effects or presence of autophagy upon anti-VEGF drug treatment of fibroblast-like cells in an *in vitro* model for CNV cellular matrix formation.

3. Materials and Methods

All experiments performed during this study complied to the Guidelines of the Helsinki Declaration and the ARVO statement for use of animals in ophthalmic and visual research, and were approved by the Regional and Institutional Research Ethics Committee at the University of Debrecen, Hungary (DE OEC: 3094–2010). The experimental animal study was approved by the Ethical Committee according to the rules of "Scientific and practical recommendations for hosting the animals and experimental work" Ministry of Health Care (Protocol #5, from 19.06.2002) and The Law of Ukraine about defending the animals from violence (№1759-VI from 15.12.2009).

3.1. Study of intravitreal drug delivery technique

3.1.1. Needles

Three types of needles were used in this study: 1) standard hypodermic 27G needle (BD™, Franklin Lakes, New Jersey, USA) with outer diameter of 0.41 mm; inner diameter of 0.21 mm; wall of 0.101 mm, and length of 13 mm (**Figure 6 A, B, C**); 2) standard hypodermic 30G needle that is regularly used for IVI (BD™, Franklin Lakes, New Jersey, USA) with outer diameter of 0.31 mm; inner diameter of 0.16 mm; wall of 0.076 mm, bevel degree 12° (A-bevel), and length of 13 mm (**Figure 6 D, E, F**).

The 27G and 30G HN have a trephine-like design of the tip with sharp inner and outer edges due to polishing of the tubes during their manufacturing (Kucklick 2006). The needles are made of stainless steel.

The third type of needle was pencil-point needle for spinal anesthesia Pencan 27G (B.Braun, Melsungen, Germany) with outer diameter of 0.42 mm; inner diameter of 0.16 mm; wall of 0.076 mm, and length of 88 mm (Apiliogullari, Duman et al. 2010). The latter needle type has a pick-like design of the tip with a side port, which margins are blunt (**Figure 6 G, H, I**). It was designed for safe single shot handling of the spinal anesthesia and diagnostic lumbar puncture that is facilitated by easy identification of passing the dura mater and arachnoid. The needle has a pencil point atraumatic tip design which protects against vascular puncture and nerve damage.

It is reported by the manufacturer that there is no tip deformation even after bone contact.

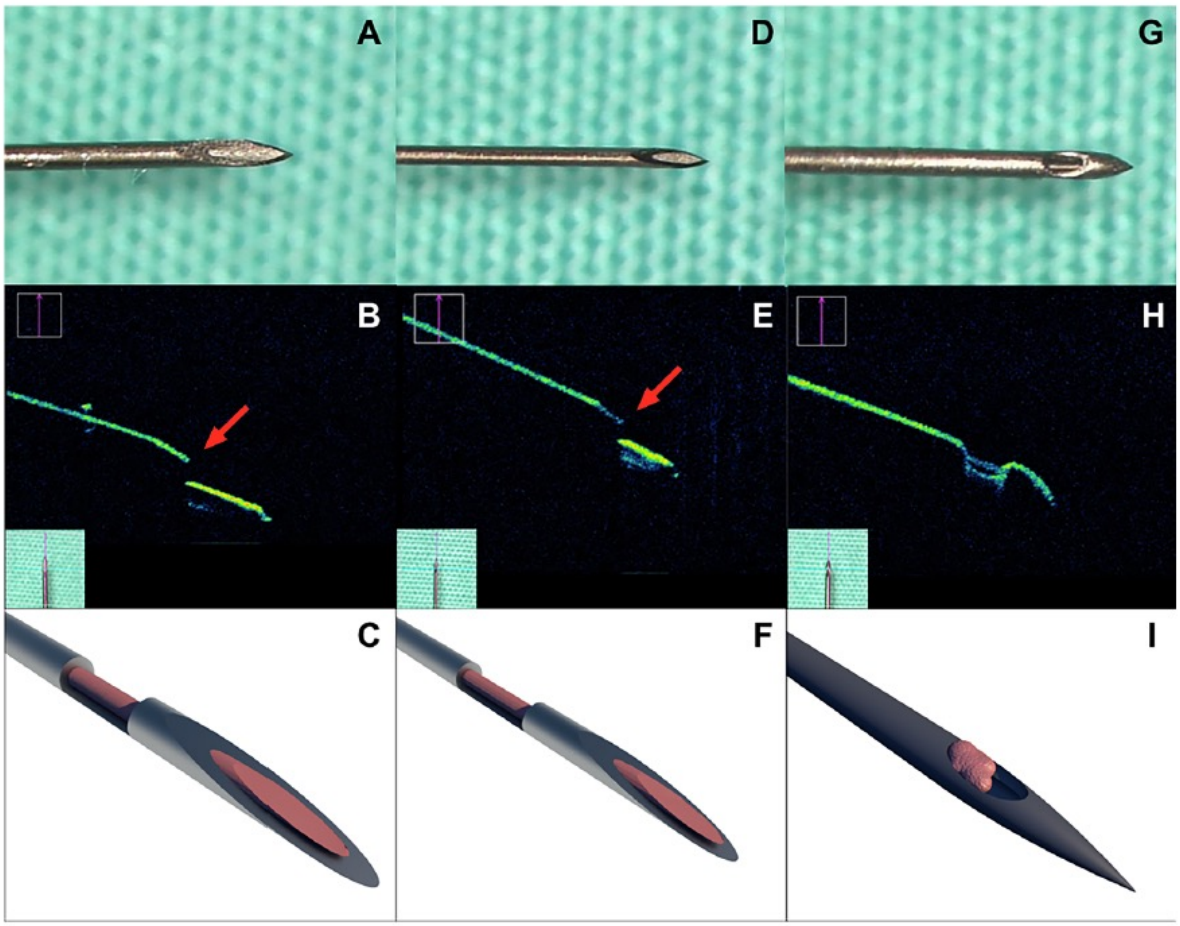

Figure 6. The needle types used in the experiments. Enlarged view of the hypodermic 27G (A), 30G (D) needles and Pencan 27G (G) needle. Intraoperative spectral domain optical coherence tomography imaging (iSD-OCT) of the hypodermic 27G (B), 30G (E) needles and Pencan 27G (H) needle. Red arrows indicate the sharp inner edge of the tip of the hypodermic needles (B, E). Schematic view of the hypodermic 27G (C), 30G (F) needles and Pencan 27G (J) needle with cellular content inside the needle's tips (pink).

The 1.0 cc syringes used in the experiments were preloaded with 0.02 cc of balanced salt solution (BSS) and connected to each needle in order to dissolve and flush out aspirated cells. Every needle was used only once.

Intraopeative spectral domain OCT (iSD-OCT) with Rescan 700 (Zeiss, Oberkochen, Germany) was used to image the tips of the needles including the inner sharp edge (**Figure 6 B, E, H**). The iSD-OCT technical data were following: volume

scans 512 x 128 cube, scan length of 6 mm: 512x128 cube, wavelength - 840 nm, iSD-OCT scans with length 6 mm, scan mode cross-hair, scanning speed - 27.000 A-scans per second, refresh rate - 5 Hz to 50 Hz, axial resolution - 5.5 μm in tissue.

3.1.2. Intravitreal penetration and aspiration on rat and human cadaver eyes

The animal study was conducted on 30 rat eyes of 30 white outbred rats (age: 6 months, weight: 600-800 g). Anesthesia was facilitated by subcutaneous injection of 0.2 mL of 1% thiopental solution and 0.4 mL of 20% oxybutirate-Na solution. Ten IVIs were performed with hypodermic 27G needles, 10 IVIs with - hypodermic 30G needles, and 10 IVIs - with spinal anesthesia Pencan 27G needles. The needles penetrated through the ciliary body 1 mm posterior to the limbus area in oblique fashion directed toward central retina under the control of operating microscope to avoid lens and peripheral retina trauma (Walker WF 1998, Smith DG 2001) (**Figure 7**). Each injection was performed on the right eye of the animal.

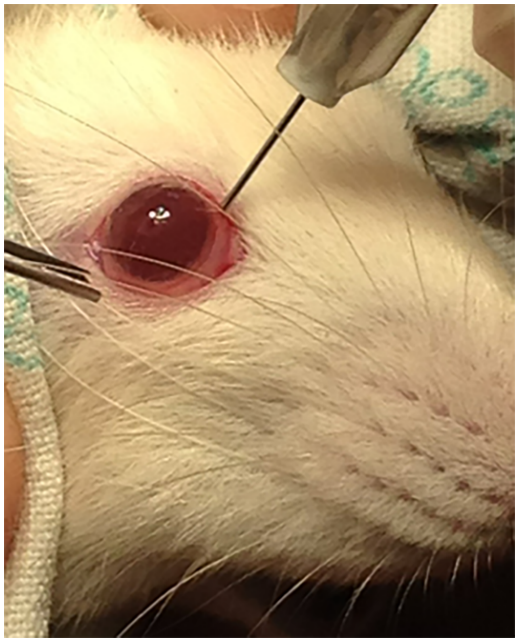

Figure 7. Performance of the IVI with 27G hypodermic needle through the ciliary body 1 mm posterior to the limbus on rat's eye under general anesthesia.

The human study was conducted on cadaver eye enucleated within 12 hours (h) from death. Only hypodermic 30G and spinal anesthesia Pencan 27G needles were used. Ten IVIs were performed with hypodermic 30G needles, and 10 IVIs - with spinal anesthesia Pencan 27G needles. Transconjunctival intravitreal penetration with

the needles into the vitreous cavity was performed perpendicularly to the sclera 4 mm posterior to the limbus.

Instead of injection, aspiration of 0.01 cc of vitreous body was performed. The procedure was performed using operating microscope in order to control the position of the needle tip and needle orifice in narrow vitreous cavity of the rat's eye. To perform IVIs with 27G Pencan needles that have the length of 88 mm, the surgeon used both hands while performing the penetration, avoiding the bending of the needle.

The corneas of the rats and cadaver eyes were marked with a linear abrasion in the meridian that corresponded to the needle's entry site for easy localization of the penetration place and adequate preparation of the paraffin blocks and sections (Walker WF 1998). In animal experiments, the euthanasia was performed at the same day after the IVI by an overdose of a 10% sodium thiopental solution.

3.1.3. Cytological study of needle tip aspirates

Aspirated material containing pre-loaded BSS was evacuated through the same IVI needle onto glass slides, where it was fixed with 4% formalin and stained with azure-2-eosin. The number of each cell type was assessed in 30 equal visual fields in the shape of equal squares of 160 μm^2. The cells were recognized by their morphological characteristics, and their quantity counted in each square of all cases studied. The cytological analysis was performed with the use of light microscope HD Microscope Camera CC50HD (Leica Mikrosysteme Vertrieb GmbH, Wetzlar, Germany) using magnification of 100X and 400X.

The study aimed to reveal and recognize the cells of ocular tissues through which the needles penetrated (conjunctiva, sclera, ciliary body, vitreous). Separate cells were counted and presented in numbers, and cellular complexes (granular proteins, conjunctival cell conglomerates) were estimated by their area of distribution in 1 mm^2. The granulated basophilic protein sediments were considered to be a result of cellular damage. Conjunctival cell complexes were the group of so called fasciated conjunctival cells, which connected with each other by intracellular junctions and were supported by a basal membrane.

3.1.4. Histological study of needle entry sites in tissues from rat and human cadaver eyes

After euthanasia of the rats, the right eyes were enucleated, and the corneo-scleral segments that corresponded to the IVI were excised and fixed in 10% formalin solution. Similar excision of the previously marked corneo-scleral segments was performed on cadaver eyes. Consequent washing and embedding of the prepared tissue samples into paraffin was used by applying a combined method with intermediate medium of 2% celloidin solution in alcohol-ether mixed at a ratio of 1:1. Slices 8 µm thick were stained with azure-2-eosin and hematoxyllin and eosin (H&E) [24]. The right eye sections in rats were compared to the left eye sections considered to be controls. The histological analysis was performed with the use of light microscope (Leica ICC50HD, Germany, magnification: 100X and 400X).

3.1.5. Cellular cultivation study

Aspirated material of cadaver eyes (n=5 per needle type per eye) were evacuated into 96 well plates containing medium consisting of Dulbecco-modified Eagle's medium nutrient mixture - F12 HAM (DMEM-F12, Sigma-Aldrich, St. Louis, MO, USA), supplemented with 20% fetal calf serum (FCS) (Gibco; Gibco, London, UK), 200 mM/mL L-glutamine (Sigma-Aldrich), 10,000 U/mL penicillin-10 mg/mL streptomycin (Sigma-Aldrich); 24 h after seeding, adherent cells were cultivated in total of 200 µL medium. Feeding of the cells occurred on each alternate day. The growth of the cells was monitored under phase contrast microscope regularly. After 4 weeks of cultivation, the cells were fixed in 4% formalin and the nuclei stained by Hoechst (1:800, 10 min). The histological analysis was performed using an EVOS FL Cell Imaging System (Thermo Fisher Scientific, Waltham, MA, USA, magnification: 40X and 100X).

3.2. Study of anti-VEGF drugs' properties *in vitro*

3.2.1. Cell culture and treatment regimes

In vitro studies were performed using a fibroblast-like mouse cell strain L_{929} obtained from ATCC® and cultivated according to conventional methods (Hay and Cohen 1989, Dyakonov 2009) and nutrient medium composed of RPMI-1640 supplemented with FCS (10%) and gentamicin (10mg/mL). Cultivation of the cell strain with different concentration of anti-VEGF drugs was performed as described below.

Ranibizumab (Lucentis, Novartis, Switzerland), a fragment of a human monoclonal antibody against VEGF-A, which is secreted by recombinant strain of Escherichia coli and its isoforms selectively bind to VEGF-A (VEGF110, VEGF121, and VEGF165), was added to the culture 24 h after fresh cell plating in concentrations of 12.5, 50, 125, and 250 μg/mL. Bevacizumab (Avastin, Genetech/Roche, USA), a monoclonal antibody against VEGF, which is used off-label to treat various eye diseases in which increased concentration of VEGF is found and NV is present, was added to the culture 24 h after fresh cell plating at concentrations of 0.65, 3.13, 6.5, and 12.5 μg/mL. Pegaptanib (Macugen, Pfizer, USA), a pegylated modified oligonucleotide that binds selectively and with high affinity to an extracellular VEGF165, was added to the culture 24 h after fresh cell plating at concentrations of 0.075, 0.15, 0.3, 0.75, and 1.5 μg/mL. Aflibercept (Eylea, Bayer Health Care, Germany), a fusion protein approved in the United States and Europe for the treatment of wet form of age-related macular degeneration, working by binding to circulating VEGF (subtypes VEGF-A and VEGF-B), as well as to placental growth factor (PGF), thus inhibiting growth of new blood vessels in the choriocapillaris (Browning, Kaiser et al. 2012), was added to the culture 24 h after cell plating at concentrations of 0.04, 0.08, 0.2, 0.4, and 0.5 μg/mL. Minimal drug concentrations were established according to the appearance of a multiplex of cellular effects (cellular proliferation, mitotic activity, polykaryocytic index, and apoptosis) and applied into the study, while maximal concentrations were determined with relevance and close approximation to the ones used in clinical practice (e.g., 0.5mg/4mL vitreous volume for ranibizumab; 1.25mg/4mL vitreous volume for bevacizumab; 0.3mg/4mL vitreous volume for pegaptanib; 2.0mg/4mL vitreous volume for aflibercept; all of the anti-VEGFs are used clinically at 1–3-month interval).

3.2.2. Cellular vital parameters

Different cellular responses were evaluated on a daily basis up to 5 days. The following cellular vital activity indices were evaluated: cellular growth/ expansion and mitotic and polykaryocytic indices (PKI). For cultivation, 5 Å~ 10^4 cells were added to the cell culture dishes covered by culture glass slides (size 16x8 mm) and filled up to 1mL of medium and then left to form monolayers within 5 days. Anti-VEGFs were added to the cultures 24 h after cell plating in different concentrations specified accordingly. The samples were fixed for analysis in 96% ethanol and then stained by

hematoxylin and eosin (H&E). The total number of cells and the count of mitoses and polykaryocytes (2 or more nuclei) were determined under optical microscope (Axioscope, Germany) at 1000x magnification within a grid area of 0.05 mm^2. Mitotic index and PKI were adjusted to 1000 cells (‰). Parallelly, cellular vital indices were evaluated within the intact cellular culture.

3.2.3. Cellular growth kinetics

Proliferative activity of cells was determined according to their growth kinetics parameters: specific growth velocity (μ), population doubling time (td), and reproduction velocity (n) at Day 5 of the observation (Freshney 1986).The specific growth velocity of the culture in phase of logarithmic growth was calculated using the formula μ = (ln$X$ − lnXo)t −1, where X is the cell quantity after certain time interval t (Day 5 of cultivation), Xo is the cell quantity on Day 1 of cultivation, and t is the time of observation (5 days of cultivation). Using specific growth velocity, population doubling time was calculated as td = ln 2/μ = 0693μ. Reproduction velocity (n) was determined using the formula n = 3.32 log(X/Xo).

3.2.4. Detection of Apoptosis and Autophagy

The level of apoptosis was determined on the same cultures in which the cellular vital indices were analyzed. The cells were first washed in phosphate buffered saline (PBS) and then detached for 10 min in trypsin and suspended again in PBS. Consequently, centrifugation (1400 rpm, 5min) and resuspension of the cells in propidium iodide (1 μ g/mL) were performed. The level of apoptosis was determined according to the number of apoptotic cells in pre-G1 phase using ductal cytofluorimeter FACStar Plus (Becton Dickinson, USA). Anti-LC3 polyclonal antibody was purchased from Novus Biologicals, USA (NB100-2220-0.1) for analysis of autophagy. Cell lysates were prepared from each condition after which equal amounts of protein were loaded onto the gel. Proteins were separated on a NuPAGE 15% Bis-Tris polyacrylamide gel and then transferred onto Immobilon-P Transfer Membrane (Millipore, IPVH00010). Membranes were blocked in Tris buffered saline containing 0.05% Tween-20 (TBS-T) and 5% non-fat dry milk (BioRad, 170-6435, 170-6531, and 100-04504-MSDS) for 1 h. After blocking, membranes were probed overnight at 4˚ C with the anti-LC3 antibody

in dilution buffer (TBS-T containing 1% nonfat dry milk), followed by 1 h incubation with a peroxidase-conjugated rat anti-rabbit secondary antibody (Sigma, A6154) for 1 h at room temperature. Peroxidase activity was detected with SuperSignal West Femto Maximum Sensitivity Chemiluminescent Substrate (Pierce, 34095) using a Lumi-Imager (Roche Diagnostics, Mannheim, Germany).

3.3. Statistical analysis

The study results obtained during experiments with the different needle types underwent statistical analysis using STATISTICA 10 software (StatSoft, Inc., OK, USA) according to the following methods: descriptive statistics, frequency tables, correlation matrices and t-test for Independent Samples. Statistical significance of the results obtained during cellular cultivation experiment was analyzed by the Student's t-test using Microsoft Excel and Biostat (Primer of Biostatistics, Version 4.03, by Stanton A. Glantz). A p-value of less than 0.05 was considered statistically significant. If not otherwise noted, all the experiments were performed three times independently.

4. Results

4.1. Study results of intravitreal drug delivery technique

4.1.1. Cytological study of needle tip aspirates

In both animal and human cadaver eye studies, the cytological analysis of the aspirates evacuated from the needle tip using three needle types demonstrated the presence of cellular material under all transconjunctival IVI procedures. The cellular material consisted of following cell types (**Figures 8** and **9**):

- conjunctival epithelial cells;
- scleral cells;
- ciliary body cells;
- vitreous body remnants.

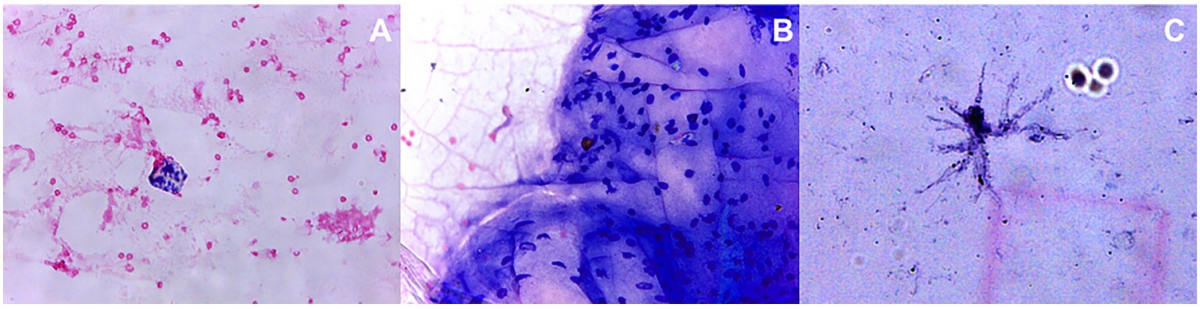

Figure 8. Aspirates taken by different needle types applied to rat eyes. Conjunctival epithelial- (A), ciliary body epithelial- (B) and sclerocyte-like cells (C) found in aspirates taken by different needles applied to rat eyes.

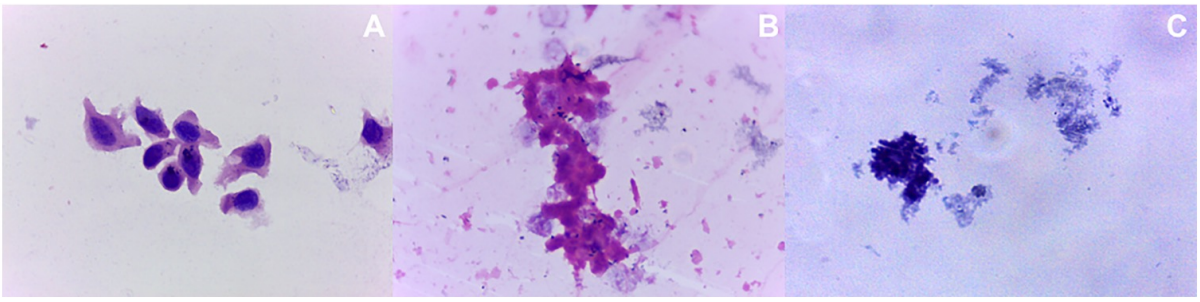

Figure 9. Aspirates taken by different needles applied to cadaver eyes. Conjunctival epithelial cells alone (A) and in complexes (B), and granular proteins (C) found in aspirates taken by different needles applied to cadaver eyes.

Moreover, the conjunctival cellular conglomerates were found amid other cells. They were presented as conjunctival epithelial cells connected to each other by intercellular junctions with or without the support from a basal membrane. The cellular content from all three needle types showed the presence of granular protein complexes, as a marker of cellular destruction. Additionally, singular erythrocytes and lymphocytes could also be noticed.

The imaging of the needle tips with iSD-OCT demonstrated the sharp inner edge of the hypodermic 27G and 30G needle tips (**Figure 6 B, C, E, F red arrows**). The Pencan 27G needle was visualized as a tip with pencil-like configuration and side port for injection (**Figure 6 H, I**).

***Animal study*.** The analysis of the absolute subtracted quantity of conjunctival epithelial cells in the cellular aspirates from hypodermic 27G needle was 56 cells, from hypodermic 30G needle – 66 cells, and for Pencan 27G needle - 170 cells (**Figure 10**).

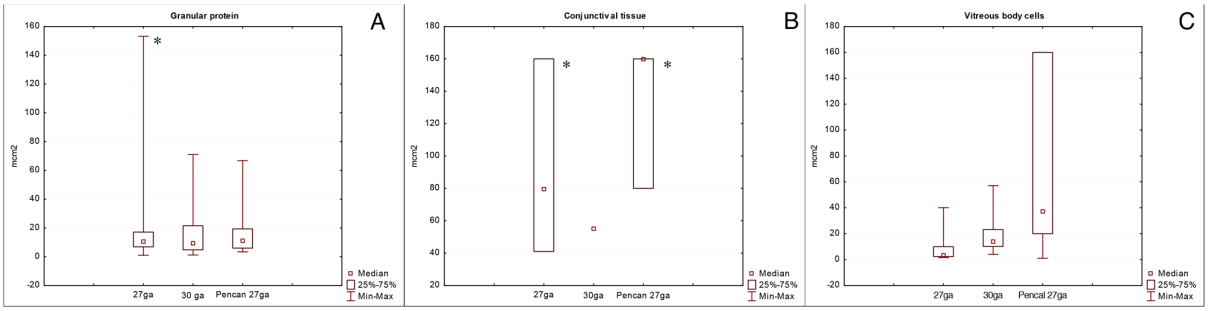

Figure 10. The amount of granular proteins (A), conjunctival cell complexes (B) and vitreous body cells (C) in the aspirates taken by different needle types applied to rat eyes. (*p<0.05).

The absolute subtracted amount of ciliary body epithelial cells in the cellular aspirates from hypodermic 27G was 69 cells, from 30G - 7 cells and from Pencan 27G needle - 136 cells. The amount of conjunctival epithelial- and ciliary body epithelial-cells was significantly higher in the Pencan 27G needle aspirates compared to the hypodermic 27G and 30G ($p = 0.05$). The absolute subtracted amount of the sclerocytes in cellular aspirates from hypodermic 27G was 24 cells, from 30G - 14 cells and from Pencan 27G needle – 17 cells. The number of sclerocytes was higher in the hypodermic 27G needles compared to the hypodermic 30G and Pencan 27G needles, with no significant difference between the last two needle types (**Figure 10**).

There were also 2 neuronal/retinal cells found in the aspirates from hypodermic 27G and 30G needles. In aspirates from the Pencan 27G needle, there were 9 cells of that particular type.

The azure-2-eosin staining showed presence of basophilic granulated sediment that represents granular proteins aggregated by the methanol fixation in all 30 aspirates taken from the needle tips after IVIs in rats (**Figure 10**). Cellular damage after IVI resulted in appearance of proteins that represent vessel exudates, connective tissue and sclera. The aspirates from hypodermic 30G and Pencan 27G needles showed significantly lower amount of granulated sediment compared to that taken from hypodermic 27G needles ($p<0.05$) (**Figure 10 A**). The amount of conjunctival cell complexes predominated in the cases where hypodermic 27G and Pencan 27G needles were used. Interestingly, the presence of basal membrane fragments attached to the conjunctival epithelial cells was noted more frequently in cellular content taken from hypodermic 27G and 30G needles, as compared to Pencan 27G needles ($p< 0.05$) (**Figure 10 B**). In each aspirate taken after IVIs with different needle types, there were a number of crystallized vitreous remnants present (**Figure 10 C**). The comparison between the different types of needles was not performed, as aspiration of the vitreous was obligatory to ensure aspiration of the cellular cylinder being cut into the syringe.

Study on human cadaver eyes. Overall, the cytological study of the needle tip aspirates taken after IVIs in human cadaver eyes revealed a less cellular material than the animal study (**Figure 11**).

The absolute subtracted quantity of conjunctival cells in aspirates from hypodermic 30G and Pencan 27G needles was 42 and 95 cells, respectively. The cytoplasm of the majority of the conjunctival cells was frothy and the nuclear margins were with poor delineation (**Figure 9 A, B**). The total square area of the granular protein complexes revealed in cellular material taken from the hypodermic 30G needles was 328.58 μm^2, and that from Pencan 27G needles was 483.32 μm^2 (**Figure 11 A, B**).

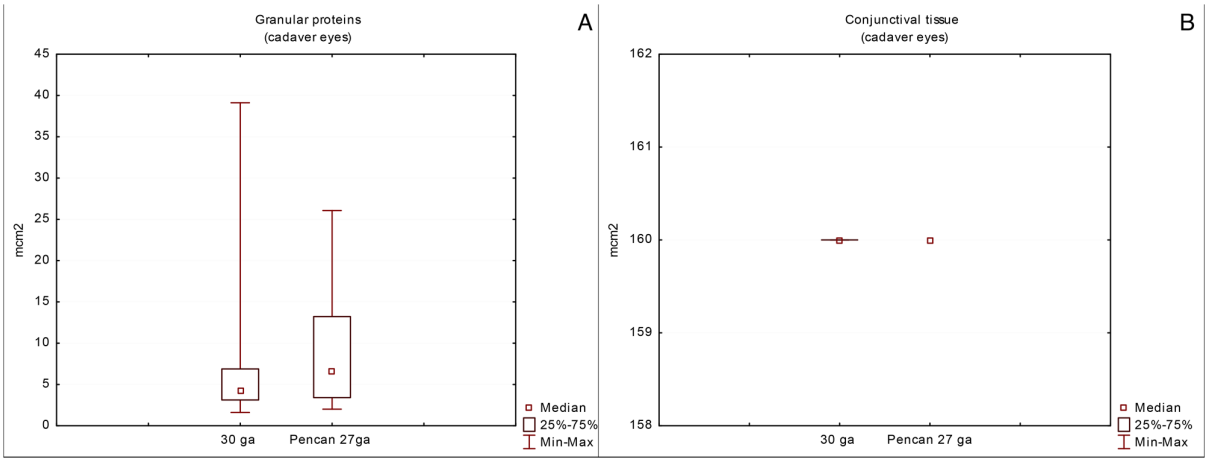

Figure 11. The amount of conjunctival cell complexes (A) and granular proteins (B) in aspirates taken by hypodermic 30G- and Pencan 27G- needles applied to cadaver eyes.

The amount of conjunctival cell complexes found in aspirates from the hypodermic 30G needles was 14, and from Pencan 27G needles it was 39 cells. On the contrary to the animal study, there were neither ciliary body epithelial cells nor sclerocytes or vitreous remnants found in the cadaveric eye samples. The difference in the amount of granular protein complexes detected in the aspirates taken from both needle types was not statistically significant.

4.1.2. Histological study of the needle entry sites

***Animal study*.** The penetration with needles of each type through the ocular tissues caused all structures of the eye wall to be surpassed and damaged. A distinct linear cut throughout all ocular tissues passed, with no alignment of the cells appearing after the needle was withdrawn was noticed in cases where IVI was performed by a hypodermic 27G or 30G needle (**Figure 12 A, B**).

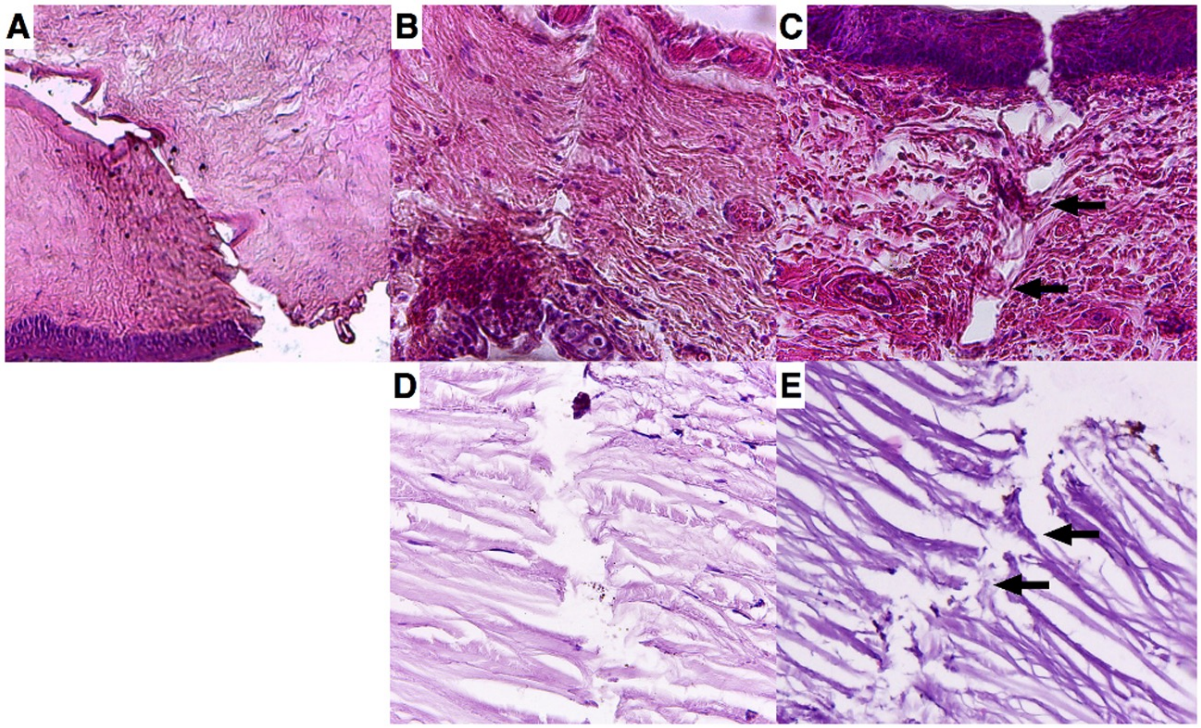

Figure 12. Histological cuts of the needle entry sites after intravitreal injection (IVI) of rat and human eyes. IVI with hypodermic 27G and 30G needles (a, b) and Pencan 27G needle (c) were performed on rat eyes. By analogy, histological cuts of the needle entry sites after IVI with hypodermic 30G needle (d) and Pencan 27G(e) on cadaver eyes is also shown. Black arrows indicate partial reposition of the collagen fibrils within the Pencan 27G needle track on rat eyes (c) and cadaver eyes (e).

All layers of tissues after the HN passage appear to be cut away and a tissue column seems to be missing after the needle withdrawal. Amid tissue changes, there were massive subconjunctival and intrascleral hemorrhages as well. The location of the hemorrhages was mostly within the needle passing track. Along this needle track, within the area of the ciliary body, there were also erythrocytes, plasmorrhagia and hemorrhage. In contrast, cases following IVI performed by the Pencan 27G needle, the cellular damage, especially that within the sclera was lesser due to a push-out effect by the pencil point tip (**Figure 12 C**). The collagen fibrils were partially torn apart, the majority of the collagen fibrils were preserved by the push-out effect of the Pencan 27G needle, and a partial filling-back effect in the needle track could be observed as well. Within the ciliary body, a similar partial filling-back effect after IVI with Pencan 27G needle could be noticed. The rate of hemorrhages seen inside the track was lower with the Pencan 27G needle type compared to the hypodermic 27G and 30G

needles, where the hemorrhages appeared to be located around the needle track in almost all cases.

Study on human cadaver eyes. The use of hypodermic 30G needle for IVIs caused a linear cut off of the eye wall tissues (**Figure 12 D**). Within the needle track, single erythrocytes could be noticed. In contrast, the needle track after IVIs with Pencan 27G needle showed the push-out effect on cadaver eye sclera. The part of the collagen fibrils appeared destroyed, when the rest was pushed out to the sides. A number of collagen fibrils was replaced back to fill in the needle track (**Figure 12 E**). Overall, the study of the entry sites on human cadaver eyes showed similar results to those found in rat eyes.

4.1.3. Cultivation of cell aspirates from human cadaver eyes *ex vivo*

The cellular material obtained from the aspirates after IVIs with hypodermic 30G and Pencan 27G needles underwent *ex vivo* cultivation in cell growth medium. The amount of cells adherent to the cell culture dish after 24 hours of seeding was significantly higher in cases of Pencan 27G (**Figure 13 G, H**) compared to the cases of hypodermic 30G needle (**Figure 13 A, B**).

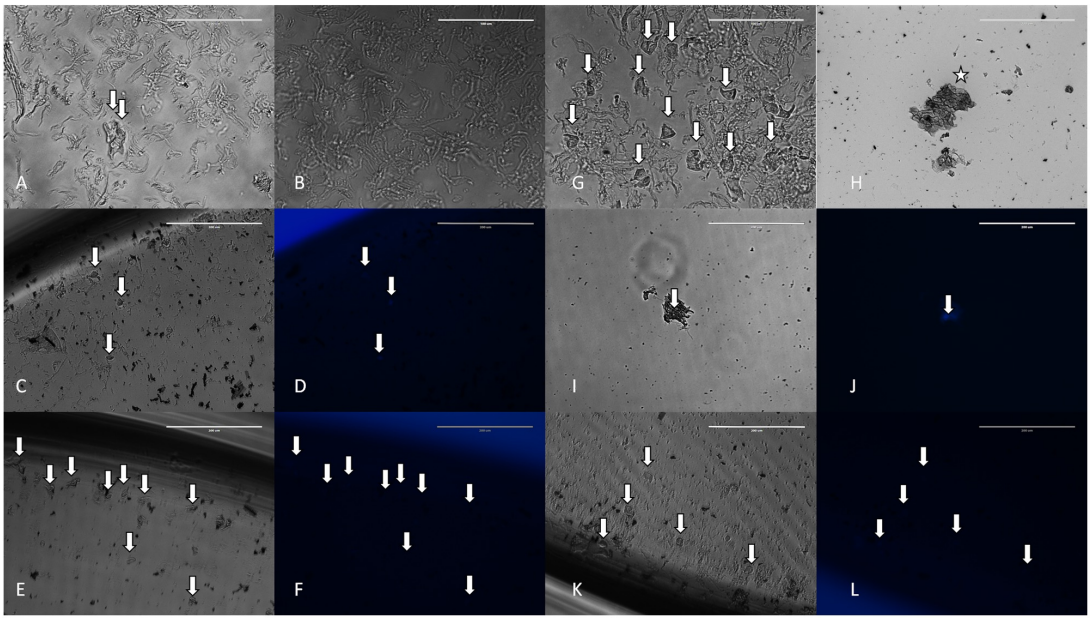

Figure 13. *Ex vivo* cultivation of cell aspirates from cadaver eyes. Cell conglomerates, single cells, vitreous remnants in hypodermic 30G (A-F) and Pencan 27G (G-L) needle aspirates of human cadaver eyes. Nuclei were stained by Hoechst (D, F, J, L). White arrows point out on cells, while the white star shows a cell aggregate. Scale bar: A, B, G, H = 100μm; C, D, E, F, I, J, K, L = 200μm.

The origin of the adherent or gravitationally immobile cells was predominantly from the conjunctiva. There were also single cells and vitreous remnants found in the cases of hypodermic 30G needle (**Figure 13 A, B**). Cultivation of the cellular content taken from 27G needle aspirates demonstrated more presence of conjunctival cell conglomerates (**Figure 13 H**). Neither ciliary body epithelial cells nor scleral cells could be found in the *ex vivo* cultures. After a 4 weeks cultivation period, among all the cell types detected, only the conjunctival cells presented signs of proliferation and could be seen in the cell culture wells (**Figure 13 C, D, E, F, I, J, K, L**).

4.2. Study results of anti-VEGF drugs' properties *in vitro*

4.2.1. Morphological and functional characteristics of intact L_{929} cellular culture

An intact fibroblast-like cell strain L_{929} was used and characterized throughout the study as a dense cellular monolayer. Morphologically, the majority of the cultured cells were polygonal- and spindle- shaped. The cellular nuclei were relatively large. The cytoplasm was vacuolated and contained small granules. There were few di- and tri-nucleated cells found in the culture. Approximately 2 to 5 cells per visual field were found at the different stages of mitosis. The characteristics of the mitotic cells were the following: round shape, small cytoplasm and hyperchromatic nuclei due to condensation of the chromatin. Proliferative activity of the intact L_{929} cells increased from Day 1 to Day 5 of cultivation (logarithmic growth phase), reaching growth plateau at Day 6 (stationary growth phase). At this time point, the density of the cellular monolayer was the highest (58.0±2.7/0.05mm^2) (**Figure 14**).

At Day 3 of cultivation, a maximum mitotic activity could be observed (166.0±7.5‰). At Day 4, a reduction of the mitotic activity was noted as a consequence of contact inhibition and reaching confluency of the cellular culture. In this study, the PKI in the intact control L_{929} cells varied between 8 and 12‰.

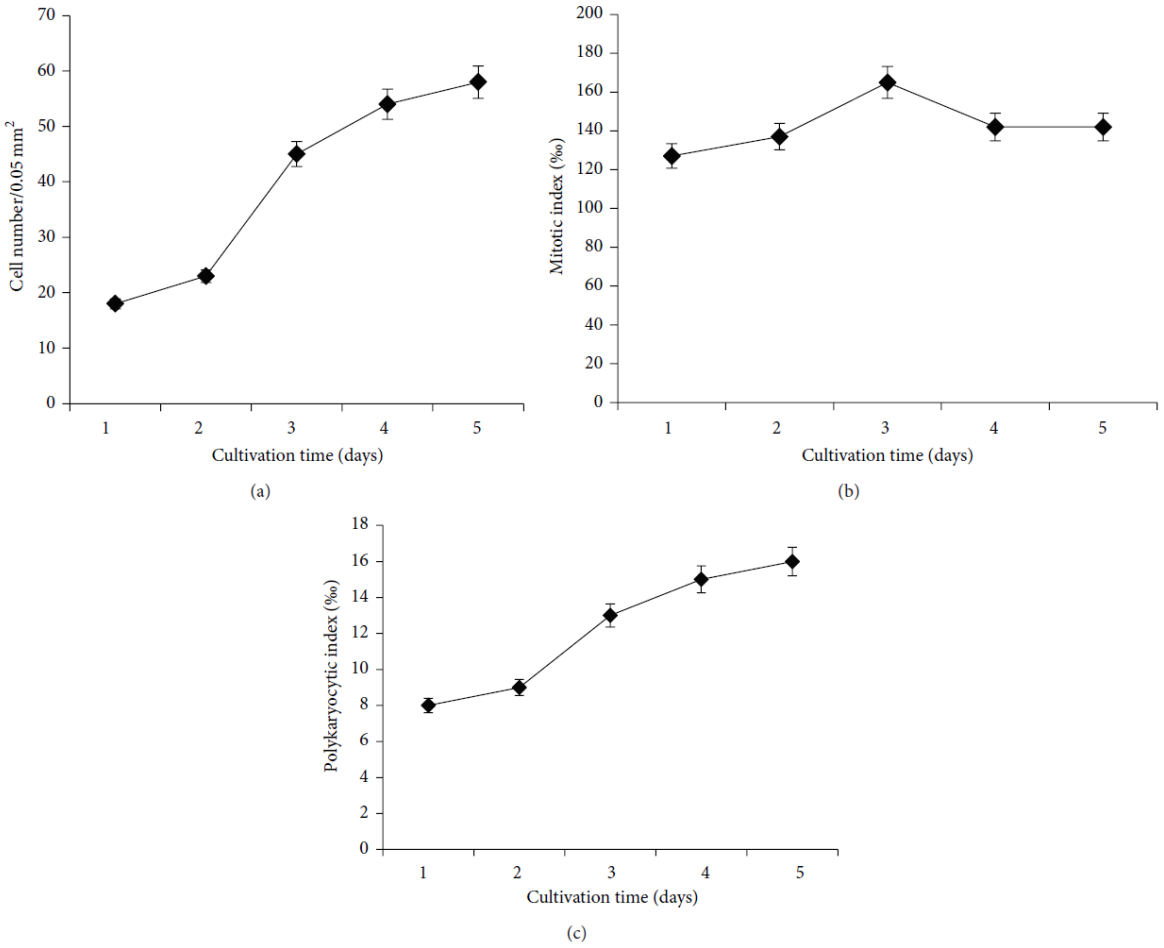

Figure 14. Kinetics of the cellular survival (A) and mitotic (B) and polykaryocytic indices (C) in untreated, control L_{929} cells.

4.2.2. Morphological and functional characteristics of L_{929} cells treated by anti-VEGF drugs

The incubation of L_{929} cells strain with four different anti-VEGF drugs in different concentrations resulted in change of vital cellular indices.

Incubation of the L_{929} cells with ranibizumab. Cultivation of the cells with ranibizumab in a concentration of 12.5 μg/mL led to a decrease in the monolayer density by 3 times (**Figures 15 A** and **16 A**).

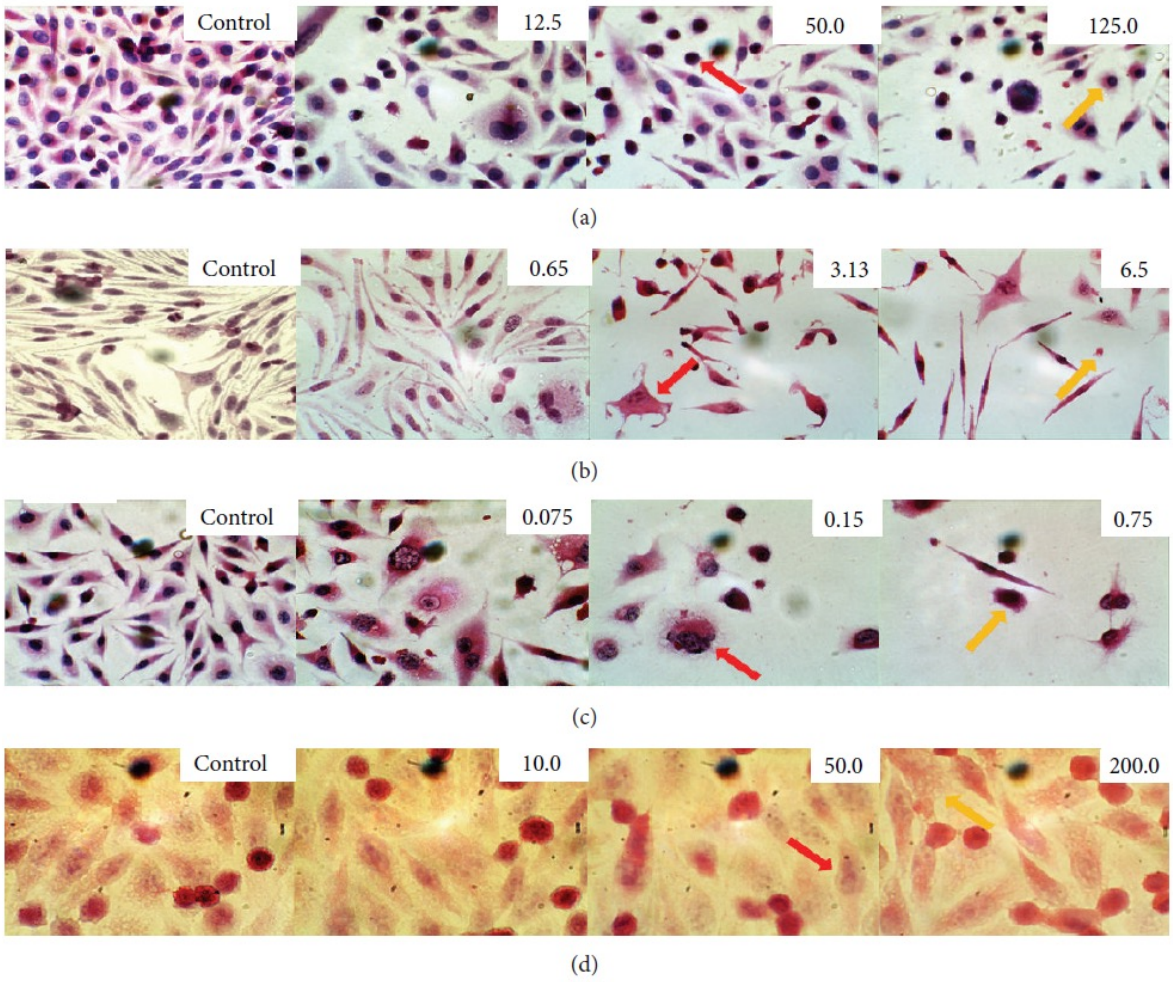

Figure 15. Cellular effects of ranibizumab (a), bevacizumab (b), pegaptanib (c), and aflibercept (d) on L_{929} cells. Cells shown are at Day 5 of various treatment concentrations (H&E staining, magnification ×1000).

This finding was associated with an increase in the number of cells with apoptotic features that included shrunk cytoplasm and condensed chromatin in the nucleus (**Figures 15 A (red arrow)** and **16 D**). The majority of the treated cells preserved their spindle-shape morphology. At the same time, the polykariocytic index (PKI) increased by 54‰ (**Figure 16 C**) demonstrating signs of cell failure. The heterogeneity of the cell culture increased further at higher concentrations up to 125.0 μg/mL, concurrent with the change in cellular morphology - mainly round and polygonal cell shapes being detected accordingly (**Figure 15 A (yellow arrow)**); the PKI increased significantly up to 62‰ under such conditions. The mitotic index remained relatively stable and did not differ much from the control (**Figure 16 B**). Incubation of the L_{929} cells at a dose of 250 μg/mL resulted in severe degradation of the cellular structure and strong vacuolization of the cytoplasm.

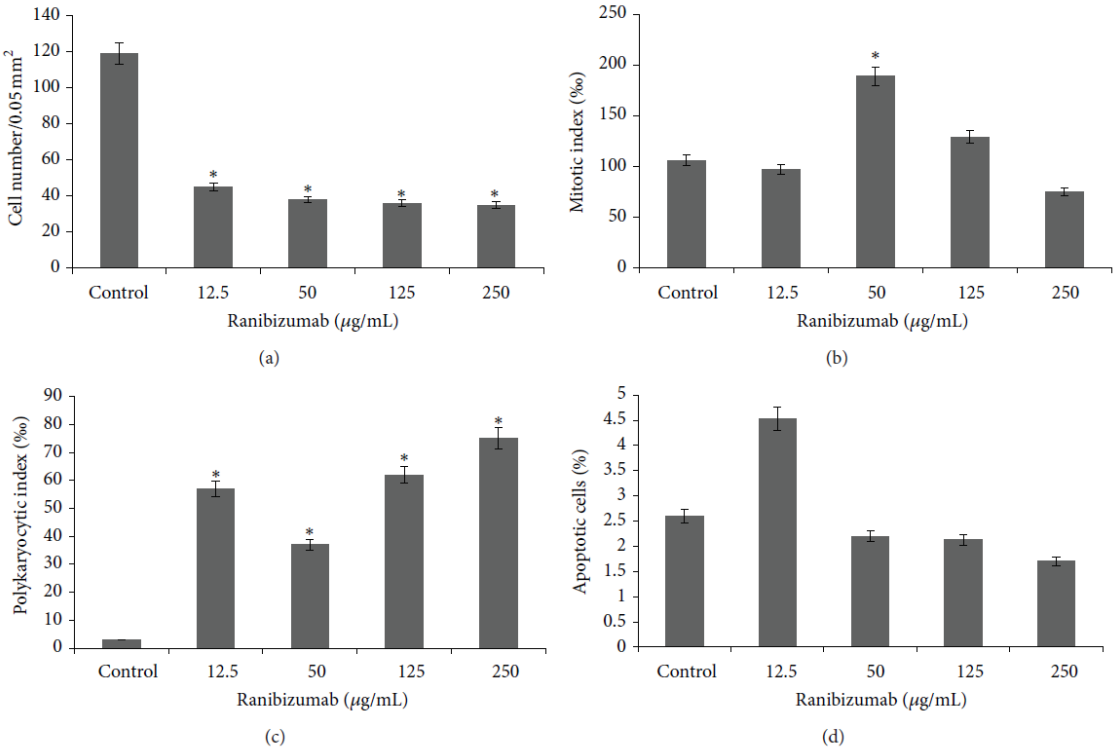

Figure 16. Kinetics of cellular proliferation (a), mitotic activity (b), polykaryocytic index (c), and apoptosis (d) in L_{929} cells treated by ranibizumab at different concentrations (data shown are at Day 5 of the treatment; n = 3, $^*P < 0.05$).

Incubation of the L_{929} cells with bevacizumab. Cultivation with bevacizumab at concentration of 0.65 μg/mL induced no morphological changes to the L_{929} cells compared to the control (**Figure 15 B**). The application of higher doses of bevacizumab up to 3.13 μg/mL induced some changes in the cell culture that were presented as increased heterogeneity of the cells with round and more prominent polygonal cellular morphology (**Figure 15 B (red arrow)**). There appeared to be a small number of mitotic cells with vacuolar cytoplasm. Additionally, an increase of 6.3 times in the number of polykaryocytes could be documented (**Figure 17 C**).

The cellular mitotic index and cell number were decreased by 1.9 and 1.6 times, respectively, for the bevacizumab treatment accordingly (**Figures 17 A** and **17 B**). Severe degradation of the cellular structures could be noticed at higher concentrations of bevacizumab (6.25 and 12.5 μg/mL, respectively). After cultivation with these concentrations, the cytoplasm appeared fully vacuolated, and a large number of apoptotic cells appeared (38.0±1.5 and 46.0±2.2, respectively) (**Figures 15 B (yellow arrow)** and **16 D**). A significant reduction in the cell density and mitotic activity as well

as increase in the PKI was noticed at concentrations higher than 0.625 μg/mL (P < 0.05) (**Figure 17 C**).

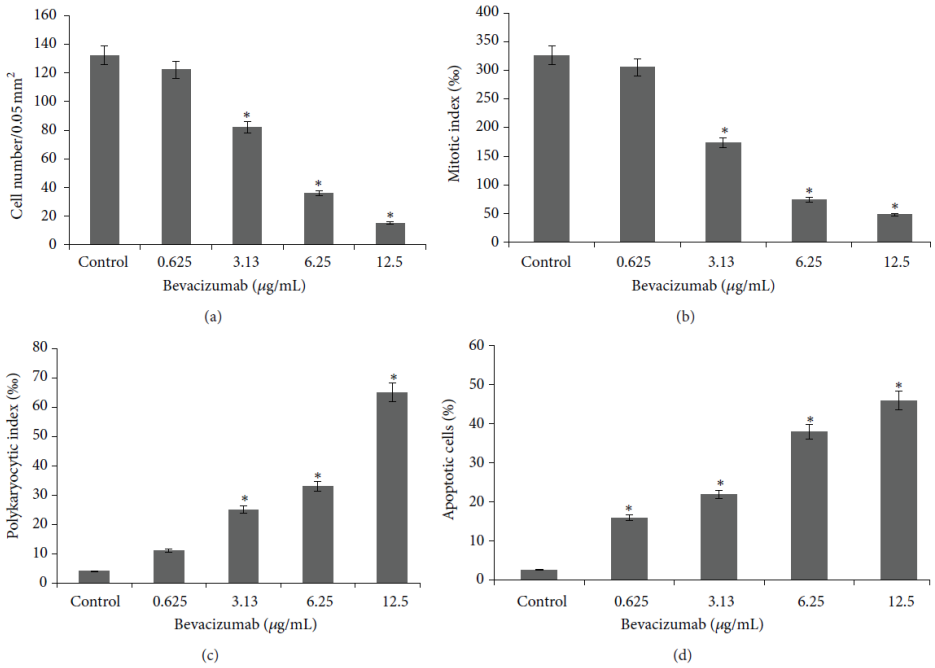

Figure 17. Kinetics of cellular proliferation (a), mitotic activity (b), polykaryocytic index (c), and apoptosis (d) in L_{929} cells treated by bevacizumab at different concentrations (data shown are at Day 5 of the treatment; n = 3, $^*P$ < 0.05).

Incubation of the L_{929} cells with pegaptanib. A significant antiproliferative effect of this drug upon the cellular culture was noticed starting from its lowest dose (0.075 μg/mL) (**Figure 18 A**).

The number of apoptotic cells in the culture was almost doubled, and a significant decrease in the cell number and mitotic activity compared to the controls could be found (P < 0.05) (**Figure 18 A, B**). The antiproliferative activity of pegaptanib escalated with the further increase in the dose up to 1.5 μg/mL, and was associated with a reduction in the density of the cells and the appearance of vacuoles in the cytoplasm (**Figure 18 C (red arrow)**). The apoptotic cells could also be detected at higher concentrations of the drug (**Figure 18 C (yellow arrow)**), however, their number, surprisingly, was similar to that of the control cell culture (**Figure 18 D**). At the same time, the number of mitoses appeared to decrease and the number of polykaryocytes to increase accordingly (**Figure 18 B, C**).

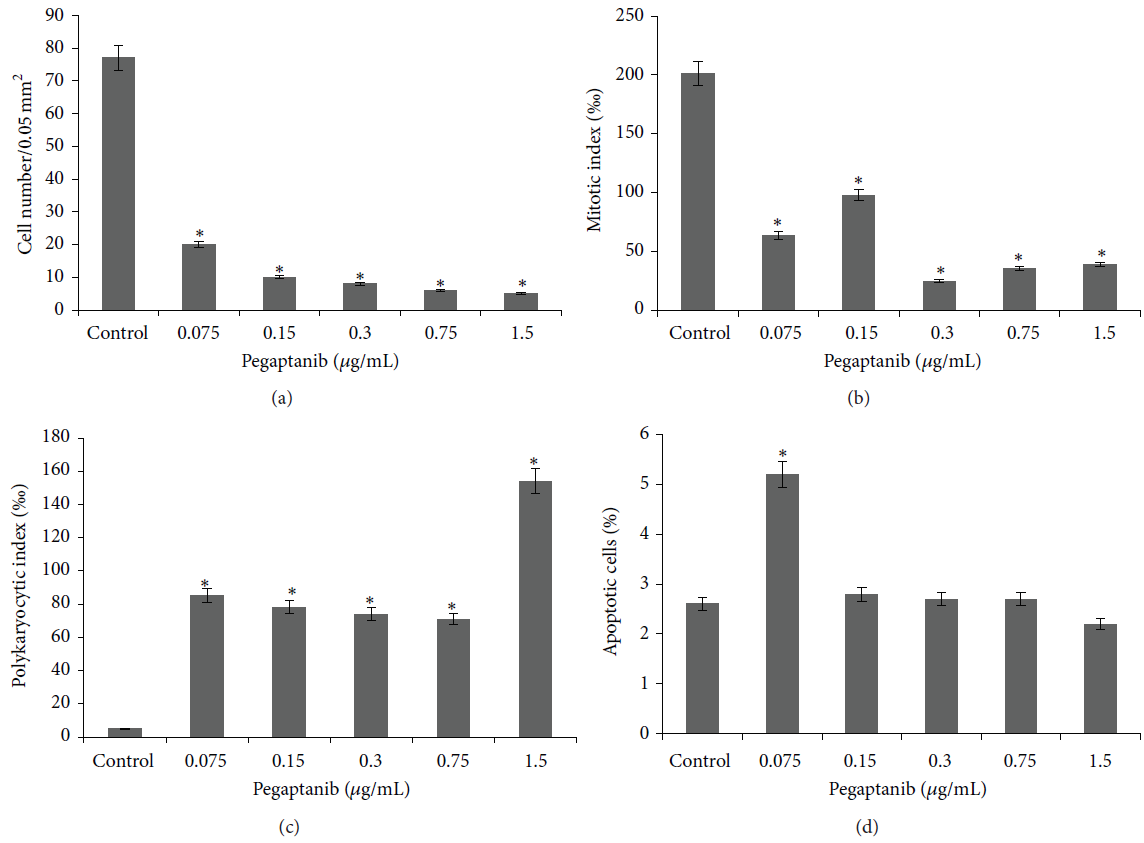

Figure 18. Kinetics of cellular proliferation (a), mitotic activity (b), polykaryocytic index (c), and apoptosis (d) in L_{929} cells treated by pegaptanib at different concentrations (data shown are at Day 5 of the treatment; n = 3, $^*P < 0.05$).

Incubation of the L_{929} cells with aflibercept. Cultivation with aflibercept showed less morphological differences in the L_{929} cells compared to the other anti-VEGFs used and to the control. The majority of the cells remained mostly polygonal and spindle shaped with centrally located well-colored round/oval nuclei (**Figure 15 D (red arrow)**). The cytoplasm was described as a well meshed structure that was mildly vacuolized (**Figure 15 D (yellow arrow)**). There were many cells at a different stage of mitosis. The formation of polykaryocytes was almost absent compared to the controls (**Figure 19 C**).

The cell number was reduced by at least 1.6-fold with drug concentration of 10 μg/mL, and by 2.2-fold with a maximum concentration of 200 μg/mL (**Figure 19 A**). The mitotic index showed no change compared to the control, and it correlated well with the morphological cellular stability observed (**Figure 19 B**).

There was no statistical difference between PKI of control cells and PKI of the cell culture cultivated with 50 or 200 μg/mL of aflibercept ($P < 0.05$). The number of

apoptotic cells (**Figure 19 D**) increased and was depended in a nonlinear manner on the drug concentration.

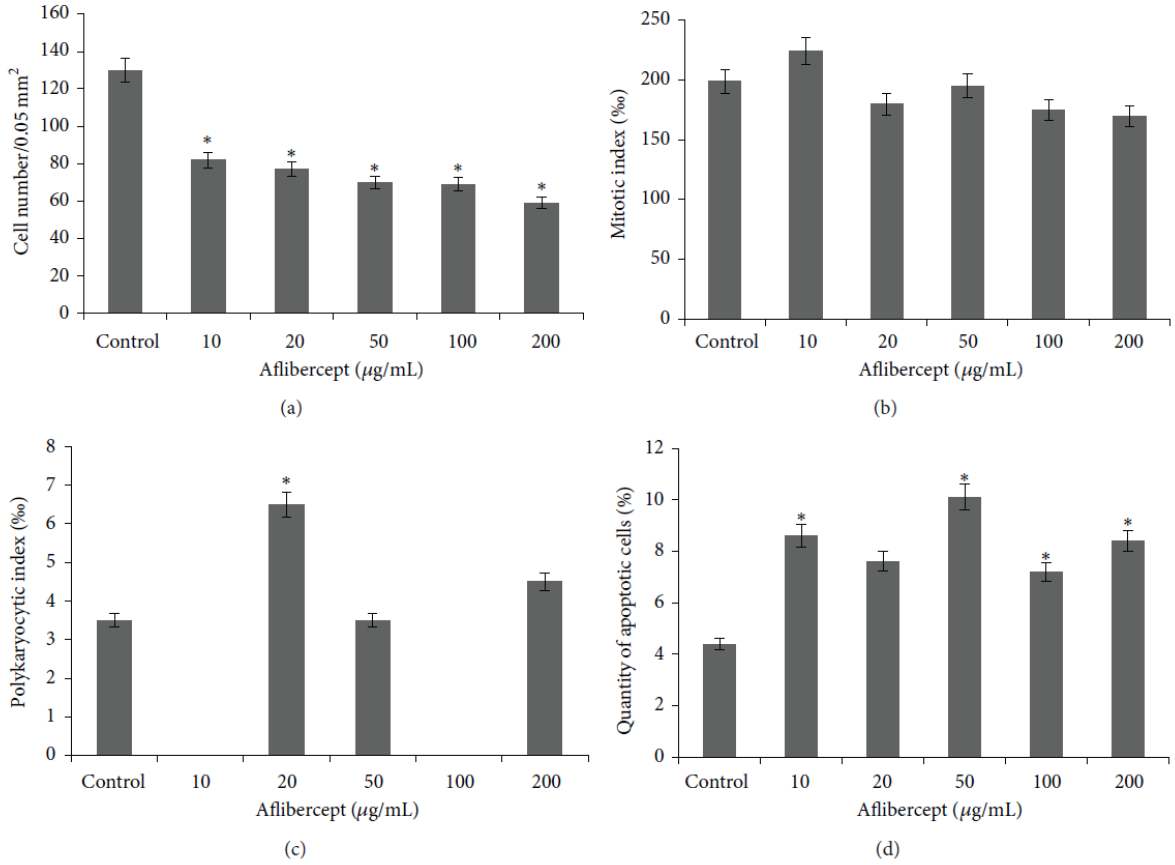

Figure 19. Kinetics of cellular proliferation (a), mitotic activity (b), polykaryocytic index (c), and apoptosis (d) in L_{929} cells treated by aflibercept at different concentrations (data shown are at Day 5 of the treatment; n = 3, $^*P < 0.05$).

4.2.3. Cellular Growth Kinetics of L_{929} Cells under Different Treatment Regimes

The cellular growth effect of the different concentrations of the four anti-VEGF drugs used in the study is demonstrated in **Figure 20**.

Analysis of the cellular growth kinetic parameters that included specific growth velocity (μ), population doubling time (td), and cell reproduction velocity (n)), showed that ranibizumab appeared to be less aggressive compared to the other three anti-VEGF drugs. It could be explained by the fact that the cellular death was compensated by the cellular reproduction (**Figure 20 A**) (Freshney 1986). In the case of bevacizumab, the minimal concentrations induced quicker cellular proliferation that

prevailed the cellular death (**Figure 20 B**). Nevertheless, this effect changed completely to the opposite under higher concentrations, which provoked generalized cell death through initiation of apoptosis. Pegaptanib activity appeared to be antiproliferative starting from the lowest concentrations. In this case, the destruction of the cells appeared to be faster than the cellular mitosis. The higher concentrations shifted the balance between survival/reproductive activity and death towards death (**Figure 20 C**). The number of cells was significantly reduced after cultivation with aflibercept (**Figure 20 D**) in concentrations of 50 to 200 μg/mL. At the same time, the population doubling time decreased (at 50 μg/mL), and the rate of cell proliferation increased. Again, the higher concentrations of the anti-VEGF drug (aflibercept) shifted the balance between survival/reproductive activity and death towards death. In this case, the cellular death was mostly induced by apoptosis.

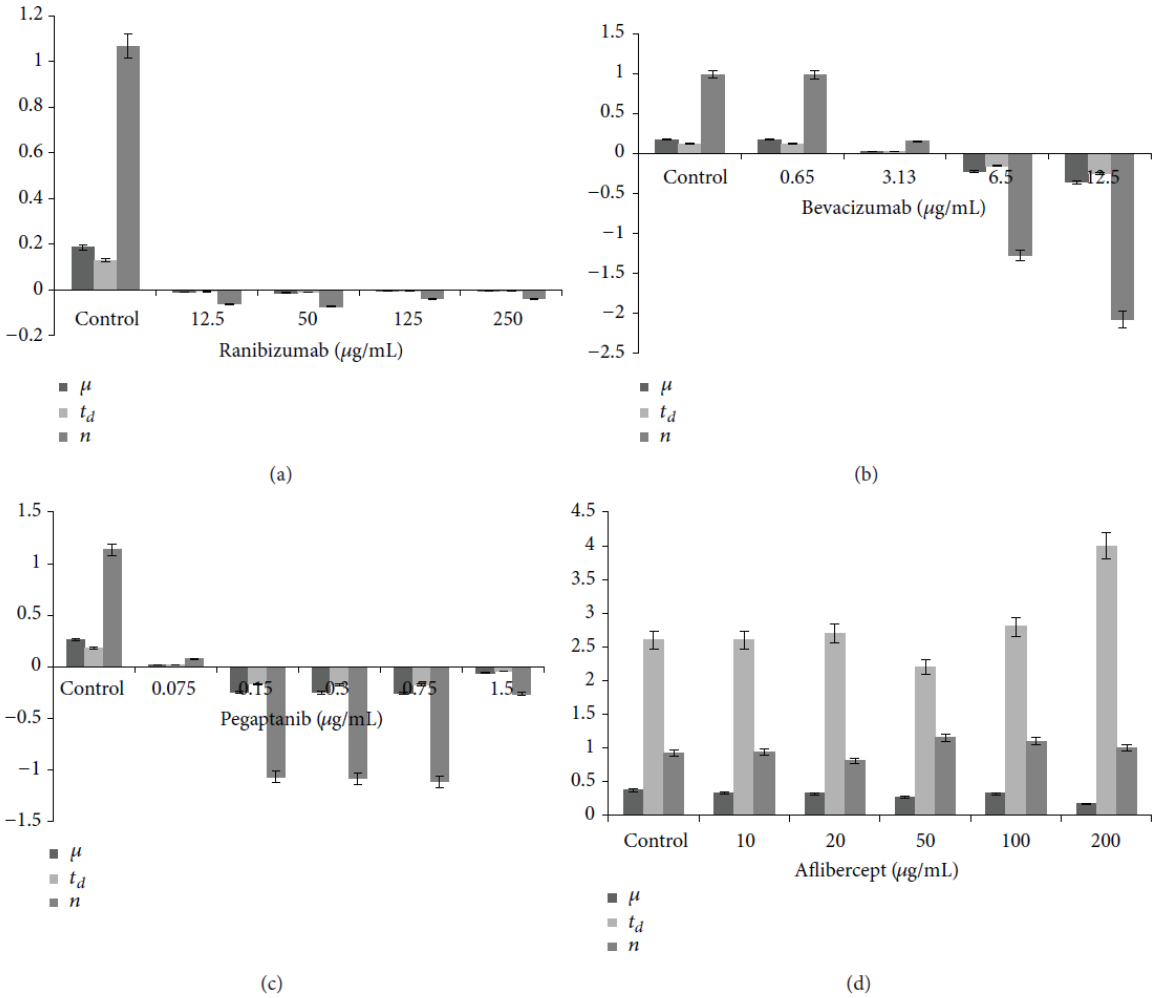

Figure 20. Comparison of the cellular growth kinetics in L_{929}. Specific growth velocity (μ), population doubling time (td), and cell reproduction velocity (n) are shown under treatment with ranibizumab (a), bevacizumab (b), pegaptanib (c), and aflibercept (d) at different concentrations (data shown are at Day 5 of the treatment; n = 3).

Cultivation of the cells with the drug in concentration of 200 μg/mL reduced the progression of cellular growth. It was considered to be a marker for the reproductive death (pathologic mitosis) and apoptosis.

4.2.4. Induction of Autophagy by Ranibizumab and Bevacizumab in L_{929} Cells

The presence of autophagy was tested for the treatments with ranibizumab and bevacizumab by the appearance of vacuoles in the cytoplasm of L_{929} cells. Both anti-VEGF drugs stimulated conversion of the cytoplasmic form of the myosin light chain kinase 3 (LC3) I into the autophagic vacuoles-bound LC3 II. Moreover, the highest concentrations of both drugs induced highest conversion of LC3 I to LC3 II (**Figure 21**).

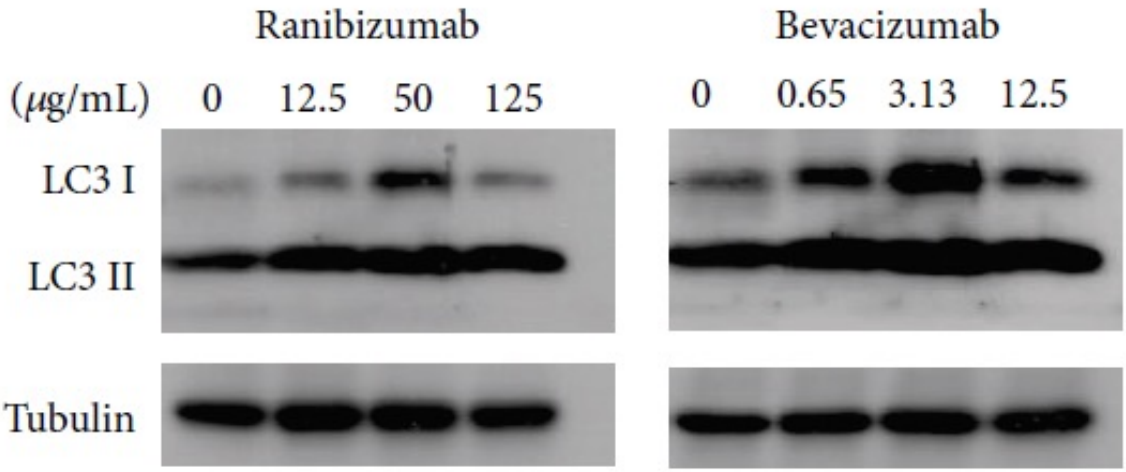

Figure 21. Induction of autophagy by ranibizumab and bevacizumab in L_{929} cells.

5. Discussion

IVIs as a surgical technique have been used since almost 100 years and primarily it was applied to the eyes with retinal detachment in order to inject a gas bubble into the vitreous cavity to tamponade the retinal tear. Later on, with the development of antibiotics, IVIs were used to treat endophthalmitis. Since nearly two decades passed since the introduction of anti-VEGF drug therapy for the treatment of proliferative ocular conditions, the number of IVIs has dramatically increased, and this approach has become the basic treatment method of ocular and, in particular, retinal diseases. For example, in 2013 in the USA, there were over 4 million IVIs performed, which rose further to almost 5.9 million injections performed in 2016. In spite of this increase, the IVI technique has been relatively unchanged, with no unique approach existing to perform the injection of the drugs. The necessity for straightforward and clear practical guidelines based on the latest evidence shall be considered or assumed in order to reduce the risks and complications that can vary from insignificant discomfort to severe complications: vitreous hemorrhage, retinal detachment and endophthalmitis. In 2004, Aiello et al. published the first consensus guidelines on IVIs (Aiello LP 2004). Since then, a number of attempts have been made to analyze the already known approaches and techniques, and to create a clear practical and unified statement (Grzybowski A. 2018). The main reason for that is the presence of nearly 28 failure modes associated with the greatest clinical risks related to IVIs, which have been discovered after a thorough assessment of the IVI use. According to such an analysis, the most dangerous and vision threatening complications with IVIs have been related to room, equipment, patient and surgeon sterility, drug preparation, injection technique and patient information (Scott and Bressler 2013). Moreover, experimental studies and ongoing pre- and clinical studies of the already existing and newly developed anti-VEGF drugs have revealed a number of new side effects, which could not be fully explained.

After introduction of anti-VEGF drugs into the treatment of chorio-retinal and vitreous pathology with increased VEGF secretion, the IVIs took its leading place among the treatment modalities and surgical drug delivery methods (Jeganathan and Verma 2009, Scott and Bressler 2013, Avery, Bakri et al. 2014, Ruiz-Moreno, Montero et al. 2015). To date, there is no unique, standard IVI protocol that has been accepted

among all or even majority of eye surgeons (Avery, Bakri et al. 2014, Fagan and Al-Qureshi 2014, Grzybowski A. 2018). The IVI technique which is usually applied all over the world uses standard hapodermic needle (HN) of different gauges to pass through the ocular tissues and distribute the drug into the vitreous cavity (Fagan and Al-Qureshi 2014). The application of HN can certainly be considered as one of the failure modes related to the equipment that is associated with occurrence of sight threatening complications. In HN, both the outer and inner edges of the needle are sharp due to the way they are manufactured (Kucklick 2006). In our study, the background hypothesis to be tested was based upon the principle of fine needle biopsy. During such procedure, which is being widely used in different medical fields, a trephine-like needle with sharp outer and inner edges is used to penetrate the tissue of interest and excise a column of the tissue which the needle passes through. The tissue column that is cut off and situated inside the needle tip is then gently aspirated and the needle is withdrawn. The cellular content of the aspirate is processed and the required study is made. The standard IVI technique with facilitation of 27G and 30G hypodermic needles in both rat and human cadaver eyes, demonstrated ocular tissue damage which differs in its extent and is dependent on the needle type. Additionally, our study shows an alternative way of IVI technique with the use of Pencan 27G spinal anesthesia needle. The results demonstrate the differences between cellular damage, aspirated cellular content and condition of the post-injection site.

The use of anti-VEGF drugs for treatment of chorio-retinal pathological conditions associated with increased production of VEGF became a gold standard therapy in the last two decades. Up-to-date, only a few studies have dedicated themselves to the study of the side effects of anti-VEGFs on intraocular tissues (Wang, Fei et al. 2004, Spitzer, Wallenfels-Thilo et al. 2006, Martin S. Spitzer 2007, Kaempf, Johnen et al. 2008, Carneiro, Falcao et al. 2009, Schnichels, Hagemann et al. 2013). The second part of this thesis work is therefore devoted to the comparison of the antiproliferative activity and different dose-dependent properties of four well known anti-VEGFs (ranibizumab, bevacizumab, pegaptanib, and aflibercept) on fibroblast-like cells *in vitro*. It is indeed the fibroblasts and the myofibroblast which are the most proliferative cells within CNVs and fibro-vascular proliferative membranes.

***Study of the needle aspirates after IVIs*.** This study confirms that the use of HN with sharp inner edges leads to the cellular damage and cut of a tissue column by the needle tip. The fact that the cellular content locates inside the needle tip before

the injection of anti-VEGF drugs, creates the high risk of cellular content being injected and disseminated into the vitreous body and probably on the surface of the inner retina.

Amid the most frequently found cells inside the needle tips were conjunctival epithelial-, ciliary body non-pigmented epithelial- and sclerocyte-like cells and vitreous body remnants. The study of the cellular aspirates taken from the alternatively used IVI Pencan 27G needle with pencil-point tip design showed a higher number of conjunctival cells, conjunctival cell complexes and ciliary body epithelial cells. Nevertheless, it shall be noted that this needle type is not designed specifically for IVI use. On the other hand, the use of Pencan 27G needle has been associated with the push-out effect applied to the ocular tissue, that facilitated less cellular damage compared to the hypodermic 27G needle, which showed presence of significantly higher amount of basophilic granulated protein sediment (a sign and a consequence of cellular damage of the microvasculature, connective and soft tissues). The histological study of the needle entry site demonstrated that during the penetration with the two different needle types, the sites of the injection had different track left by each needle. In the cases with hypodermic (27G and 30G) needles, the needle tip made a cut off a tissue column. In contrast to HN, the needle tip of the Pencan 27G spinal anesthesia needle pushed the cells aside and assumed partial re-positioning of the cells within the needle track after the needle was withdrawn. The results of the *ex vivo* cultivation of the cells obtained from the needle tip aspirates (hypodermic 30G and Pencan 27G needles) showed a gradual adherence and slight proliferation of conjunctival cells within 24 h and up to 4 weeks. These data can serve as a proof of a hypothetical growth of the injected cells in the vitreous cavity and/or the retinal inner surface.

Another clinical problem that occurs during IVI is the presence of pain of different grade and a vitreous reflux, which extent correlates with the needle size (van Asten, van Middendorp et al. 2015). It was reported, that even if 33G needle is applied, the occurrence of pain compared to the 30G needle does not become reduced, due to presence of mainly associated psychological factors (pain expectation, previous IVI experience, individual pain tolerance and pre- and post-IVI aseptic measurements). With the thinner needles, however, it was possible to reduce the vitreous reflux (Hubschman, Coffee et al. 2010, De Stefano, Abechain et al. 2011). De Stefano et al. reported that during the study of the size of the scleral wound (the entry site) after IVI,

the needles with bigger gauge (thinner diameter) induced less ocular damage, and tunneled incisions showed self-sealing properties more often (De Stefano, Abechain et al. 2011). In our study, we focused on the histological analysis and comparison of the entry sites using standard HN and spinal anesthesia needle designed to penetrate the thick tissues without cutting. The results clearly demonstrated the cutting properties of the HN, producing a cut off column of all tissues being surpassed, and leaving a tissue defect on the eye wall after the withdrawal. This condition serves as a predisposing factor for vitreous reflux and risk of vitreous contamination. The histological samples of the entry sites following penetration by the pencil-like Pencan 27G spinal anesthesia needle, on the other hand, presented a partial sparing and back positioning of the cells within the needle track.

Recently it was published that the 33G needle needs less force in order to penetrate the sclera compared to 30G needles, even though the difference shown was quite insignificant (Pulido, Zobitz et al. 2007, van Asten, van Middendorp et al. 2015). Similar results were observed during our study, where the performance of the IVIs with the hypodermic 27G and Pencan 27G required a bigger force. Moreover, the needle tip aspirates from the hypodermic 27G and Pencan 27G (needles with bigger diameter) presented with a higher number of cellular contents, compared to the hypodermic 30G needle. The Pencan 27G needles with much longer tip and a relatively big side port have been designed for spinal anesthesia, but not IVIs. This can explain the fact that the trauma of the eye wall cause by such needles is relatively bigger compared to the standard HN used for IVI. We assumed that the big side port of the Pencan 27G needle is responsible for catching a bigger number of cells during the aspiration including conjunctival complexes and vitreous strands. In contrast to the Pencan 27G needle, the HN with the same diameter induced larger damage to the cellular wall of every tissue it surpassed. This is why a significantly larger amount of granulated proteins could be detected in the needle tip aspirates after IVIs with hypodermic 27G needles. The greater number of conjunctival complexes including basal membrane in aspirates taken after IVIs with HN compared to Pencan 27G needles can be explained by the distinct cutting properties of the former needle type. A septic contamination of the needles used for IVI has been studied by de Caro et al. (de Caro, Ta et al. 2008). The authors demonstrated a septic contamination of the vitreous cavity occurs even in cases when prophylaxis with antibiotics and povidone iodine have been used. The coagulase-negative *Staphylococci* strain could be isolated

in the same patients following a standard IVI from the needle tips and from bulbar conjunctival samples at the injection site. The authors suspected there was direct injection of the bacteria that inhabitate the ocular surface with further distribution of the infectious agents into the vitreous cavity through the injection needles. There was no clear explanation, however, of the mechanism of bacterial entry into the vitreous cavity (de Caro, Ta et al. 2008). Our study demonstrates that during standard IVI, there is a high probability for ocular tissues cells (including ocular surface cells) that are cut by the inner sharp edge of the standard HN to become captured inside the tip's canal and then primarily injected into the vitreous cavity and before injection of the anti-VEGF drugs. The difference in the entry site construction after the use of different needles is hereby presented as well. The HNs cut the penetrating tissues leaving a traceable and less self-sealing pathway which could be the main cause of the vitreous reflux. The pencil-point needle showed different penetration properties from those by the HNs. The cells inside the track appeared to be pushed out or to the side within the needle pathway, with a partial back positioning of the cells presumably after the needle was evacuated or retracted. To the best of our knowledge, there is no special needle for IVIs. That is why a further study of the penetrating properties of the different needle types relative to the IVIs is needed, and a new design of the needle tip has to be considered aiming to minimize or avoid the injection of the cut out cells into the vitreous cavity, and improving the self-sealing properties of the wound after the IVI.

The results of the current study allow us to establish a robust hypothesis that cellular material cut by the HN during each IVI in each patient finally is injected into the vitreous cavity. The consequences of this event, including the risks and the further role of injected cells together with the drug, have to be taken into consideration. Thus, there are two probable mechanisms of vitreous contamination during or/and after IVI that can come alone or in combination:

1. Intraoperative injection of contaminated cellular material (mainly from the ocular surface) that has been cut by the HN;
2. Postoperative contamination of the vitreous through the reflux associated needle entry site.

The second mechanism of contamination can occur after IVI in different time intervals.

Three main inflammatory events can be differentiated as the result of injected cellular material that can take place in the vitreous body:

1) aseptic reaction;

2) septic reaction;
3) autoimmune reaction;

Moreover, the hypothesis that injected cells have the ability to proliferate and grow inside the vitreous body and/or onto the inner ocular surface was supported by the following study data:

- the presence of conjunctival cellular complexes supported by a basal membrane;
- an adherence and slow proliferation and growth of cells taken from the aspirates and cultivated in growth medium *in vitro*.

The use of an alternative technique with Pencan 27G needles that have been designed for spinal anesthesia were tested and discussed further in our study. This type of needle has a pencil-point atraumatic tip, which protects against vascular puncture and nerve tissue damage. Our study showed that the amount of conjunctival epithelial cells and ciliary body epithelial cells (including conjunctival complexes and aspirated vitreous remnants) with such needle is notably higher compared to HNs ($p = 0.05$). We assumed that this difference occurred as a result of the bigger diameter of the side orifice compared to the orifice of the HNs. Additionally, in order to accomplish a penetration through the ocular tissues with the Pencan 27G needle, the use of both hands and a bigger force applied is required for IVI delivery.

There are some study limitations that shall be mentioned and explained:

1. A limitation of the cadaver eyes study: the ocular tissues in the cadaver eye demonstrated a different tissue response to the IVI compared to the living tissues of the rats' eyes.
2. The cytological study of the needle tip aspirates in the cadaver eyes demonstrated presence of cellular content in lesser quantity, which could be taken as another limitation of the cadaver eye study. We assume that it occurred due to the more appropriate size of the eye globe as compared to the rat eyes, and due to a more specific reaction of cadaver eye tissue to IVI as described above. In spite that the rat eye study and the human cadaver eye study showed different amount of cellular content in the needle tip aspirates, the distribution of the cut cells within the cellular content aspirated by the needle tips corresponded in both studies.
3. The surgical part of the study methods can also be a limitation. Standard IVI injection technique does not require an aspiration maneuver after

penetration of the eye wall with the needle. However, in order to analyze the cellular content of the needle tips, the aspiration of the vitreous was necessary, aiming to get the cells that were cut by the needle edges into the syringe. As hypothesized, after each IVI, there is a high probability that the cellular content can be injected into the vitreous cavity, with a chance for further spreading. We did not perform a study of the injected cellular material collected from the vitreous. However, the collection of the injected cells from the vitreous cavity in the experimental conditions could be reasonable and at the same time a challenging process.

4. We performed *in vitro* cultivation of the cellular material obtained from the needle tips. It might be another limitation of the study which is related to the cultivation of cells in media *in vitro* but not under the real conditions found in the vitreous. There is a possibility that proliferation of the aspirated cells in the vital vitreous *in vivo* can differ from that *in vitro*.

In general, a bigger number of sclerocyte-like cells and cellular complexes were found in samples form the hypodermic 27G needles. This type of needles caused a bigger damage to the cells of the eye wall as well, which was demonstrated by the higher amount of granular proteins. A smaller number of cells and cellular complexes was revealed in aspirates taken from the hypodermic 30G needles. This needle type presented with smaller amount of granular proteins, compared to the hypodermic 27G and Pencan 27G needles. Our data assume that the further utilization of hypodermic 27G needles for IVI has to be reconsidered.

Study of the antiproliferative activity of anti-VEGF drugs revealed certain side properties of the analyzed medicaments that probably shall be further studied and the data shall be applied to the clinical conditions.

The study results demonstrated that all four analyzed anti-VEGFs exhibited antiproliferative activity on the fibroblast-like cell strain L_{929} over a 5-day study period. The heterogeneity of the cellular monolayer increased after the cultivation with the drugs starting from the lowest concentrations. The anti-VEGFs indeed impacted the cellular viability through depression of cellular mitosis and survival, and activation of apoptosis. These effects did intensify after the increase of the concentration of each of the four anti-VEGF drugs. Moreover, concentration-dependent antiproliferative and apoptotic effects of all anti-VEGFs were documented using growth kinetic analysis

with minimally prominent effects after cultivation of cells with ranibizumab. In case of ranibizumab, the increase of concentration led to activation of cellular reproduction, meaning the concentration-dependent cellular growth was partially compensated by cellular reproduction. This data assumes that ranibizumab poses less aggressive antiproliferative activity than the other three anti-VEGFs.

The comparison of antiproliferative and cytotoxic effects of bevacizumab, pegaptanib, and ranibizumab on different ocular cells was reported recently (Martin S. Spitzer 2007). This study did not include analysis of the anti-VEGFs on fibroblast-like cells. It showed, however, that ranibizumab can reduce the cell proliferation of choroidal epithelial cells (CECs) by 44.1%, bevacizumab – by 38.2%, and pegaptanib - by 35.1%. This difference was found not to be statistically significant. In addition, the study performed on adult retinal pigment epithelium (ARPE19 cell line) demonstrated a minor antiproliferative effect of bevacizumab and pegaptanib. On the contrary, ranibizumab did not show similar activity on cell proliferation of ARPE19 cells and demonstrated no cytotoxic activity on retinal ganglion cells (RGC5), CECs, and ARPE19 cells altogether. Analysis of the ranibizumab activity showed it could efficiently block cellular migration, but not proliferation of the retinal endothelial cells. In another study, the authors compared the side effects of ranibizumab, pegaptanib, and bevacizumab on the different stages of angiogenesis on human umbilical vein endothelial cells (HUVEC) (Carneiro, Falcao et al. 2009). The data showed ranibizumab and bevacizumab can markedly increase the level of apoptosis of the HUVEC. These two anti-VEGF drugs when used in clinical doses can significantly reduce the cellular proliferation without signs of cytotoxicity at different concentrations. Additionally, incubation of HUVECs with anti-VEGFs revealed that the expression of the active form of the VEGF receptor-2 decreases by 66% in case of bevacizumab, and by 86% in case of ranibizumab and pegaptanib compared to the VEGF receptor-2 expression in control cultures. A comparison of the data from cytotoxicity and antiproliferative activity studies of aflibercept, bevacizumab, and ranibizumab on different ocular cells (ARPE19, RGC-5, and 661W) (Schnichels, Hagemann et al. 2013) showed that aflibercept does not affect cellular viability and does not induce cellular apoptosis. Aflibercept demonstrated a slight upregulating and downregulating effects on certain VEGF-related factors. Nevertheless, in comparison to bevacizumab and ranibizumab, these effects appeared not to be significant.

The results of our experimental study showed the cellular exposure effects of four different anti-VEGF drugs upon fibroblast-like cell strain L_{929} chosen as a model of the fibroblast-based cellular matrix of CNV *in vitro*. The results demonstrate the effect of anti-VEGF drugs on the proliferative activity and vital indices, including survival, proliferative and mitotic activity, apoptosis and their concentration dependence. It shows that the small concentration of anti-VEGF drugs (ranibizumab 12.5 μ g/mL, bevacizumab 3.13 μ g/mL, pegaptanib 0.15 μ g/mL, and aflibercept 0.04 μ g/mL) present a pronounced antiproliferative effect on the L_{929} cells. Within the four anti-VEGFs, only bevacizumab increased the apoptosis of L_{929} cells in all concentrations used. The reproductive cellular death of L_{929} cell culture was proven by the inhibition of the cellular proliferation and increased heterogeneity of these cells under anti-VEGFs exposure. Bevacizumab, pegaptanib, and aflibercept showed a marked dose-dependent antiproliferative effects on the L_{929} cells, which increased with increasing the dose. On the contrary, after incubation with ranibizumab, there appeared to be a compensation of the antiproliferative and apoptotic drug action by a cellular proliferation despite the increase in the anti-VEGFs concentration used. A self-digestive or self-recycling mechanism found in L_{929} cells and considered to be the sings of true autophagy could explain partially the compensatory cellular proliferation.

The L_{929} cell strain was chosen for this study as this strain does not poses a background VEGF secretion. In this condition, it was possible to analyze the alternative and/or side cellular effects of anti-VEGF drugs as an *in vitro* model for fibroblast-like cells that belong to the cellular matrix of CNVs. The fibroblasts and myofibroblasts of the CNV cellular matrix are among the most highly proliferating cell types (Scupola, Ventura et al. 2004). Additionally, L_{929} cell strain allowed to evaluate the cellular effects of different anti-VEGF drugs upon almost any similar type of vital cells with highly proliferating properties. There is a lack of data regarding the presence of VEGF receptors on the cellular membrane of fibroblast-like cells in CNV. However, it has been published there is a VEGF receptor presence on joint fibroblasts extracted from humans, as well as expression of VEGF due to inflammatory stimulation of fibroblast-like cells that can infiltrate the joint in a collagen-induced arthritis (Lu, Kasama et al. 2000).

The experimental type used in this study can be a limitation in itself, as it is difficult to apply directly the *in vitro* data to clinical conditions, such as the influence of anti-VEGF drugs upon fibroblast-like cells of CNV. However, the antiproliferative and

apoptotic activity of anti-VEGF drugs on fibroblast-like cells can explain an alternative mechanism of their action on such cell types found in CNV (Scupola, Ventura et al. 2004).

The possible inhibition of the cellular survival and mitosis by application of ranibizumab, bevacizumab, pegaptanib, and aflibercept in different concentrations and the dose-dependent effects shall be taken into consideration while using these drugs during IVI of patients. Ranibizumab alone exhibited the least antiproliferative activity on the cellular strain studied, which allowed for compensation of apoptosis by increased cellular proliferation. Cultivation with aflibercept at concentrations of 10 and 100 μg/mL showed complete absence of polykaryocytes, which may indicate the influence of the drug on the signal transfer from the membrane to the nucleus.

6. Summary

The IVI technique with the use of hypodermic or spinal anesthesia needles leads to damage of all eye wall layers on its way (conjunctiva, sclera, ciliary body). The risk of cellular structures' being captured by the needle orifice is high and can lead to injection of autologous, and/or contaminated cellular material into the vitreous cavity. Our data support the hypothesis that the sharp circumferential inner edge of standard hypodermic needles routinely used for IVI, can cut out a number of cells as shown in rat and cadaver eyes. The diameter of the needle plays a role in the severity of tissue damage and appropriate drug distribution. Additionally, the needle tip design determines the configuration of the entry site and possible vitreous reflux, respectively. Overall, our study supports the finding that hypodermic 30G needles cause less tissue damage compared to hypodermic 27G and Pencan 27G needles. Nevertheless, the role of the cellular content that is being injected into the vitreous cavity together with the drugs during under an IVI procedure has to be taken into consideration to better understand the post-injection inflammatory reaction.

Inhibition of the cellular survival and mitosis by anti-VEGF drugs (ranibizumab, bevacizumab, pegaptanib, and aflibercept) in different concentrations need to be taken into consideration as well while using these drugs in patients. Only ranibizumab, amid all anti-VEGFs studied, exhibited slightest antiproliferative activity, which allows for compensation of apoptosis by increased proliferation. The complete absence of polykaryocytes after cultivation of L_{929} cells with aflibercept at concentrations of 10 and 100 μg/mL, may indicate the influence of this drug upon the signal transfer pathway from the membrane to the nucleus.

The identified properties of the anti-VEGF drugs require further investigation of their action *in vitro* and *in vivo*. Additionally, further research pertaining to concentration-dependence of the anti-VEGFs needs to be performed to eliminate the possible side effects on healthy retinal tissues.

7. References

Aiello LP, B. A., Chang S, Cunningham ET Jr, D'Amico DJ, Flynn HW Jr, Grillone LR, Hutcherson S, Liebmann JM, O'Brien TP, Scott IU, Spaide RF, Ta C, Trese MT. Evolving guidelines for intravitreous injections. Retina. Oct;24(5 Suppl): S3-19. DOI: 10.1097/00006982-200410001-00002. PMID: 15483476.

Apiliogullari S, Duman A, Gok F, Akillioglu I. Spinal needle design and size affect the incidence of postdural puncture headache in children. Paediatr Anaesth. 2010; 20(2):177±82. https://doi.org/10.1111/j. 1460-9592.2009.03236.x PMID: 2001513925.

Avery RL, Bakri SJ, Blumenkranz MS, Brucker AJ, Cunningham ETJ, D'Amico DJ, et al. Intravitreal injection technique and monitoring: updated guidelines of an expert panel. Retina. 2014; 34:S1±S18. https://doi.org/10.1097/IAE.0000000000000399 PMID: 25489719

Bhatt SS, Stepien KE, Joshi K. Prophylactic antibiotic use after intravitreal injection: effect on endophthalmitis rate. Retina. 2011; 31(10):2032±6. https://doi.org/10.1097/IAE.0b013e31820f4b4f PMID: 21659941

Biswas P, Sengupta S, Choudhary R, Home S, Paul A, Sinha S. Comparative role of intravitreal ranibizumab versus bevacizumab in choroidal neovascular membrane in age-related macular degeneration. Indian Journal of Ophthalmology, vol. 59, no. 3, pp. 191–196, 2011.

Braun. http://www.bbraun.com/cps/rde/xchg/bbrauncom/hs.xsl/products.html?prid=PRID00000630 (accessed 14/06/2016).

Brodie FL, Ruggiero J, Ghodasra DH, Hui JZ, VanderBeek BL, Brucker AJ. Volume and composition of reflux after intravitreal injection. Retina. 2014; 34(7):1473±6. https://doi.org/10.1097/IAE.0000000000000098 PMID: 24451925

Browning DJ, Kaiser PK, Rosenfeld PJ, Stewart MW. Aflibercept for age-related macular degeneration: a gamechanger or quiet addition? American Journal of Ophthalmology, vol. 154, no. 2, pp. 222–226, 2012.

Carneiro A, Falcao M, Pirraco A, Milheiro-Oliveira P, Falcao-Reis F, Soaresa R. Comparative effects of bevacizumab, ranibizumab and pegaptanib at intravitreal dose range on endothelial cells. Experimental Eye Research, vol. 88, no. 3, pp. 522–527, 2009.

Cheung CSY, Wong AWT, Lui A, Kertes PJ, Devenyi RG, Lam W-C. Incidence of Endophthalmitis and Use of Antibiotic Prophylaxis after Intravitreal Injections. Ophthalmology. 2012; 119(8):1609±14. https://doi.org/10.1016/j.ophtha.2012.02.014 PMID: 22480743

De Caro JJ, Ta CN, Ho H-KV, Cabael L, Hu N, Sanislo SR, et al. Bacterial contamination of ocular surface and needles in patients undergoing intravitreal injections. Retina. 2008; 28(6):877±83. https://doi.org/10.1097/IAE.0b013e31816b3180 PMID: 18536606

De Stefano VS, Abechain JJK, de Almeida LFS, Verginassi DM, Rodrigues EB, Freymuller E, et al. Experimental investigation of needles, syringes and techniques for intravitreal injections. Clin Experiment Ophthalmol. 2011; 39(3):236±42. https://doi.org/10.1111/j.1442-9071.2010.02447.x PMID: 20973898

Diago T, Mccannel CA, Bakri SJ, Pulido JS, Edwards AO, Pach JM. Infectious endophthalmitis after intravitreal injection of antiangiogenic agents. Retina.

2009; 29(5):601±5. https://doi.org/10.1097/IAE. 0b013e31819d2591 PMID: 19357558

Dyakonov LP (Ed.). Animal Cells in Culture (Methods and Application of Biotechnology), Sputnik, Moscow, Russia, 2009.

Fagan XJ, Al-Qureshi S. Intravitreal injections: a review of the evidence for best practice. Clin Experiment Ophthalmol. 2013; 41(5):500±7. https://doi.org/10.1111/ceo.12026 PMID: 23078366

Fintak DR, Shah GK, Blinder KJ, Regillo CD, Pollack J, Heier JS, et al. Incidence of endophthalmitis related to intravitreal injection of bevacizumab and ranibizumab. Retina. 2008; 28(10):1395±9. https://doi.org/10.1097/IAE.0b013e3181884fd2 PMID: 18827737

Forrester JV, Docherty R, Kerr C, Lackie JM. Cellular proliferation in the vitreous: the use of vitreous explants as a model system. Invest Ophthalmol Vis Sci. 1986; 27(7):1085±94. PMID: 3721786

Freshney I. Animal Cell Culture: A Practical Approach, IRL Press Oxford, Washington, DC, USA, 1986.

Friedman DA, Lindquist TP, Mason JOI, McGwin G. Needle contamination in the setting of intravitreal injections. Retina. 2014; 34(5):929±34. https://doi.org/10.1097/IAE.0000000000000067 PMID:24509487

Goldberg RA, Shah CP, Wiegand TW, Heier JS. Noninfectious Inflammation After Intravitreal Injection of Aflibercept: Clinical Characteristics and Visual Outcomes. Am J Ophthalmol. 2014; 158(4):733±7.e1.https://doi.org/10.1016/j.ajo.2014.06.019 PMID: 24983791

Grisanti S, Ziemssen F. Bevacizumab: off-label use in ophthalmology. Indian Journal of Ophthalmology, vol. 55, no. 6, pp. 417–420, 2007.

Hay H and Cohen J. Studies on the specificity of the L929 cell bioassay for the measurement of tumor necrosis factor. Journal of Clinical and Laboratory Immunology, vol. 29, pp. 151–155, 1989.

Hubschman J-P, Coffee RE, Bourges J-L, Yu F, Schwartz SD. Experimental model of intravitreal injection techniques. Retina. 2010; 30(1):167±73. https://doi.org/10.1097/IAE.0b013e3181b094cf PMID: 19779317

Jeganathan VSE, Verma N. Safety and efficacy of intravitreal anti-VEGF injections for age-related macular degeneration. Curr Opin Ophthalmol. 2009; 20(3):223±5. https://doi.org/10.1097/ICU. 0b013e328329b656 PMID: 19367163

Jonas JB, Spandau UH, Rensch F, Von Baltz S, Schlichtenbrede F. Infectious and noninfectious endophthalmitis after intravitreal bevacizumab. J Ocul Pharmacol Ther. 2007; 23(3):240±2. https://doi. org/10.1089/jop.2006.0146 PMID: 17593007

Kaempf S, Johnen S, Salz AK, Weinberger A, Walter P, Thumann G. Effects of bevacizumab (avastin) on retinal cells in organotypic culture. Investigative Ophthalmology & Visual Science, vol. 49, no. 7, pp. 3164–3171, 2008.

Karcioglu ZA. Fine needle aspiration biopsy (FNAB) for retinoblastoma. Retina. 2002; 22(6):707±10.PMID: 12476095

Klein KS, Walsh MK, Hassan TS, Halperin LS, Castellarin AA, Roth D, et al. Endophthalmitis After Anti-VEGF Injections. Ophthalmology. 2009; 116(6):1225-.e1. https://doi.org/10.1016/j.ophtha.2009.02.031 PMID: 19486799

Kucklick TR. Introduction to Needles and Cannulae. Kucklick TR, editor. Boca Raton, FL 33487±2742: CRC. Press Taylor and Francis Group; 2006. 90±8 p.

Kumaran N, Sim DA, Tufail A. Long-term remission of myopic choroidal neovascular membrane after treatment with ranibizumab: a case report. Journal of Medical Case Reports, vol. 3, article 84, 2009.

Lu J, Kasama T, Kobayashi K. Vascular endotelial growth factor expression and regulation of murine collageninduced arthritis," Journal of Immunology, vol. 164, no. 11, pp. 5922–5927, 2000.

Natividad A, Freeman TC, Jeffries D, Burton MJ, Mabey DCW, Bailey RL, et al. Human Conjunctival Transcriptome Analysis Reveals the Prominence of Innate Defense in Chlamydia trachomatis Infection. Infect Immun. 2010; 78(11):4895±911. https://doi.org/10.1128/IAI.00844-10 PMID: 20823212

Ojcius DM, Souque P, Perfettini J-L, Dautry-Varsat A. Apoptosis of Epithelial Cells and Macrophages Due to Infection with the Obligate Intracellular Pathogen Chlamydia psittaci. J Immunol. 1998; 161 (8):4220±6. PMID: 9780196

Pulido JS, Zobitz ME, An KN. Scleral penetration force requirement for commonly used intravitreal needles. Eye. 2006; 21(9):1210±1. https://doi.org/10.1038/sj.eye.6702577 PMID: 16946745

Rodrigues EB, Grumann AJ, Penha FM, Shiroma H, Rossi E, Meyer CH, et al. Effect of needle type and injection technique on pain level and vitreal reflux in intravitreal injection. J Ocul Pharmacol Ther. 2011; 27(2):197±203. https://doi.org/10.1089/jop.2010.0082 PMID: 21314588

Ruiz-Moreno JM, Montero JA, Araiz J, Arias L, GarcõÂa-Layana A, Carneiro A, et al. Intravitreal anti-vascular endothelial growth factor therapy for choroidal neovascularization secondary to pathologic myopia: six years outcome. Retina. 2015; 35(12):2450±6. https://doi.org/10.1097/IAE.0000000000000632 PMID: 26049616

Schnichels S, Hagemann U, Januschowski K et al. Comparativetoxicity and proliferation testing of aflibercept, bevacizumab and ranibizumab on different ocular cells. British Journal of Ophthalmology, vol. 97, no. 7, pp. 917–923, 2013.

Scott AW, Bressler SB. Long-term follow-up of vascular endothelial growth factor inhibitor therapy for neovascular age-related macular degeneration. Curr Opin Ophthalmol. 2013; 24(3):190±6. https://doi. org/10.1097/ICU.0b013e32835fefee PMID: 23492430

Scupola A, Ventura L, Tiberti AC, D'Andrea D, Balestrazzi E. Histological findings of a surgically excisedmyopicchoroidal neovascular membrane after photodynamic therapy. A case report," Graefe's Archive for Clinical and Experimental Ophthalmology, vol. 242, no. 7, pp. 605–610, 2004.

Sigford DK, Reddy S, Mollineaux C, Schaal S. Global reported endophthalmitis risk following intravitreal injections of anti-VEGF: a literature review and analysis. Clin Ophthalmol. 2015; 9:773±81. https://doi. org/10.2147/OPTH.S77067 PMID: 25999685

Smith DG, Schenk MP. Dissection Guide & Atlas to the Rat. Edition 1 ed. Colorado, USA: Morton Publishing Company; 2001.

Spitzer MS, Wallenfels-Thilo B, Sierra A et al. Antiproliferative and cytotoxic properties of bevacizumab on different ocular cells. British Journal of Ophthalmology, vol. 90, no. 10, pp. 1316–1321, 2006.

Spitzer MS, Yoeruek E, Sierra A et al. Comparative antiproliferative and cytotoxic profile of bevacizumab (Avastin), pegaptanib (Macugen) and ranibizumab (Lucentis) on different ocular cells. Graefe's Archive for Clinical and Experimental Ophthalmology, vol. 245, no. 12, pp. 1837–1842, 2007.

Van Asten F, van Middendorp H, Verkerk S, Breukink MB, Lomme RMLM, Hoyng CB, et al. Are intravitreal injections with ultrathin 33-G needles less painful than the commonly used 30-G needles? Retina. 2015; 35(9):1778±85. https://doi.org/10.1097/IAE.0000000000000550 PMID: 25901838

Van der Reis MI, La Heij EC, De Jong-Hesse Y, Ringens PJ, Hendrikse F, Schouten JSAG. A systematic review of the adverse events of intravitreal anti-vascular endothelial growth factor injections. Retina. 2011; 31(8):1449±69. https://doi.org/10.1097/IAE.0b013e3182278ab4 PMID: 21817960

Walker WF, Homberger DG. Anatomy and Dissection of the Rat (Freeman Laboratory Separates in Biology). 3rd edition ed 1998.

Wang Y, Fei D, Vanderlaan M, Song A. Biological activity of bevacizumab, a humanized anti-VEGF antibody in vitro. Angiogenesis, vol. 7, no. 4, pp. 335–345, 2004.

8. List of publications of the author

Publications related to this Thesis:

Lytvynchuk L, Sergienko A, Savytska I, Albert R, Glittenberg C, Binder S, Petrovski G. Comparative cyto-histological study of needle tip aspirates and entry sites after intravitreal injection using different needle types. PLoS One. 2017 Jul 10;12(7): e0174467.

Lytvynchuk L, Sergienko A, Lavrenchuk G, Petrovski G. Antiproliferative, Apoptotic, and Autophagic Activity of Ranibizumab, Bevacizumab, Pegaptanib, and Aflibercept on Fibroblasts: Implication for Choroidal Neovascularization. J Ophthalmol 2015:934963.

Other publications:

Lytvynchuk L, Glittenberg C, Binder S (2017) Intraoperative Spectral Domain Optical Coherence Tomography: Technology, Applications, and Future Perspectives. In: Meyer CH, Saxena S, Sadda SR (eds.) Spectral Domain Optical Coherence Tomography in Macular Diseases. Springer, New Dehle, India, pp 423-443.

Lytvynchuk LM, Glittenberg CG, Falkner-Radler CI, Neumaier-Ammerer B, Smretschnig E, Hagen S, Ansari-Shahrezaei S, Binder S. Evaluation of intraocular lens position during phacoemulsification using intraoperative spectral-domain optical coherence tomography. J Cataract Refract Surg. 2016 May;42(5):694-702.

Lytvynchuk LM, Falkner-Radler CI, Krepler K, Glittenberg CG, Ahmed D, Petrovski G, Lorenz B, Ansari-Shahrezaei S, Binder S. Dynamic intraoperative optical coherence tomography for inverted internal limiting membrane flap technique in large macular hole surgery. Graefes Arch Clin Exp Ophthalmol. 2019 Aug;257(8):1649-1659. doi: 10.1007/s00417-019-04364-5.

Lyubomyr M. Lytvynchuk MD, PhD, Christiane I. Falkner-Radler, Andrzej Grzybowski MD, PhD, Carl G. Glittenberg MD, Farnusch Shams-Mafi MD, Siamak Ansari-Shahrezaei MD, Susanne Binder MD. Influence of optic media of the human eye on the imaging of Argus® II retinal prosthesis with intraoperative spectral-domain optical coherence tomography. Spektrum für Augenheilkinde (Austria, Vienna) DOI: 10.1007/s00717-019-0429-x

L. Lytvynchuk, D. Kuhn, M. Sander, B. Lorenz (2019) Preparing Pediatric Cataract Patients for BIL Cataract Surgery. In: Marie-José Tassignon, Sorcha Ní Dhubhghaill, Luc Van Os (ed.) Innovative Implantation Technique: Bag-in-the-Lens Cataract Surgery. Springer Nature Switzerland AG, pp 197-206

L. Lytvynchuk, B. Lorenz (2019) Visual Outcomes and Complications After BIL in the Paediatric Population. In: Marie-José Tassignon, Sorcha Ní Dhubhghaill, Luc Van Os (ed.) Innovative Implantation Technique: Bag-in-the-Lens Cataract Surgery. Springer Nature Switzerland AG, pp 207-225.

L.Lytvynchuk, M.Thiele, W.Schmidt, B.Lorenz. Precision of bag-in-the-lens intraocular lens power calculation in different age groups of pediatric cataract patients: report of the Giessen Pediatric Cataract Study Group. Journal of Cataract & Refractive Surgery.DOI: https://doi.org/10.1016/j.jcrs.2019.05.032. Published online: May 31, 2019

L.Lytvynchuk, M.Thiele, B.Lorenz. Analysis and management of intraoperative and early postoperative complications of bag-in-the-lens intraocular lens implantation in different age groups of paediatric cataract patients: report of the Giessen Paediatric Cataract Study Group. Acta Ophthalmol 2019 Aug 17. doi: 10.1111/aos.14229. [Epub ahead of print]

Ruban A, Lytvynchuk L, Zolnikova A, Richard G. Efficiency of the Hydraulic Centripetal Macular Displacement Technique in the Treatment of Traumatic Full-Thickness Macular Holes. Retina 2017 Nov 7. Second first author.

Lyubomyr M. Lytvynchuk, Andrzej Grzybowski, Birgit Lorenz, Siamak Ansari-Shahrezaei, Susanne Binder. New Scleral Depressor-Marker for Retinal Detachment Surgery Ophthalmology. Retina 2019 Jan;3(1):73-76. doi: 10.1016/j.oret.2018.08.005.

9. Acknowledgments

I would like to acknowledge my supervisor ***Professor Goran Petrovski*** for his continuous support, excellent professional mentorship, and inspiration during my work and in my personal life as well. I am grateful for the opportunity to train and work in his team, and for his faith in me from the first time when we met. After many successful hard years, he showed to me the professionalism and prosperous research style and switched me back on the right way of science.

I also want to thank ***Professor Andrea Facskó***, the former Head of the Department of Ophthalmology (University of Szeged) during the period of my PhD studies for giving me the opportunity to work in her department of scientific excellence.

I would like to thank all the past and current members of the department and the Stem Cell and Eye Research Laboratory led by Professor Petrovski in Debrecen and Szeged for their help and kindness. Special thanks to for the excellent technical and laboratory assistance; and the friendly environment as well. I am thankful to my previous mentors ***Professor Andrii Sergienko, Professor Galina Lavrenchuk, Professor Susanne Binder*****,** and collaborators ***Iryna Savytska, Réka Albert, Carl Glittenberg*****,** for their excellent work and helping me during our studies.

Additionally, I would like to thank ***Stephanie Kreiling*** from University Hospital Giessen and Marburg GmbH (Giessen, Germany) for her assistance during formatting of my PhD Thesis.

And last, but not least I am sincerely grateful to my whole family and to all of my dear friends helping me get through the difficult times, and for their patience, understanding, emotional support and encouragement during my PhD years.